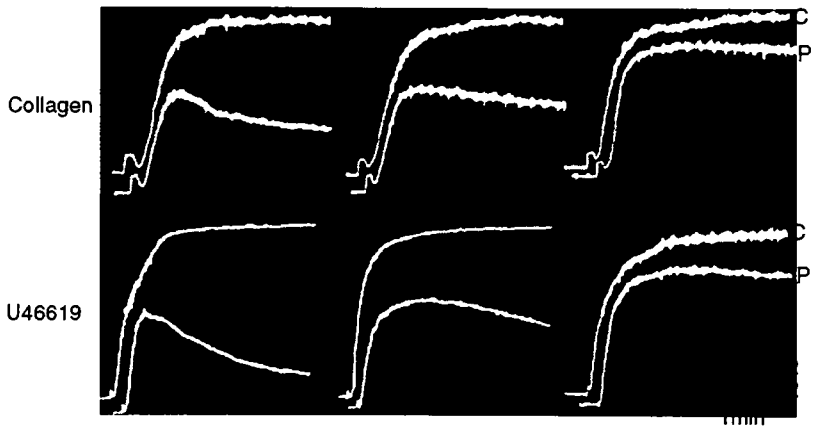

Fig. 2. Platelet aggragation induced by collagen or U46619 at various concentrations. Platelet aggregation in citrated PRP from patient OSP-1 (labeled 'P') or a control subject (labeled 'C') was induced by various concentrations of collagen or U46619. At high concentrations of collagen or U46619, OSP-1 platelets aggregate almost normally.

antagonist, did not induce an additional inhibition on the platelet aggregation (Fig. 1C). These data suggest that the impaired response of the patient's platelets may be due to an abnormality in signaling evoked by ADP and that $P2Y_{12}$-mediated signaling rather than $P2Y_1$-mediated signaling may be completely defective in patient OSP-1.

We also examined the aggregation of OSP-1 platelets induced by higher concentrations of agonists. As shown in Fig. 2, the aggregation response of OSP-1 platelets improved as the concentrations of agonists increased, and they aggregated almost normally in response to high concentrations of collagen (5 $\mu g\ mL^{-1}$), U46619 (5 μM), or PAR1 TRAP (100 μM) (not shown). In addition, we confirmed that 1 μM of AR-C69931MX conferred essentially the same defect on the aggregation of control platelets in response to U46619 as that of OSP-1 platelets and did not further inhibit OSP-1 platelet aggregation induced by 5 $\mu g\ mL^{-1}$ of collagen, 5 μM of U46619, or 100 μM of PAR1 TRAP (data not shown). These data indicated that at high concentrations of agonists OSP-1 platelets showed the specifically impaired aggregation to ADP.

Effect of ADP on PGE_1-stimulated cAMP accumulation in platelets

To determine whether $P2Y_{12}$-mediated signaling is specifically impaired, we examined an inhibitory effect of ADP on 1 μM of PGE_1-stimulated cAMP accumulation in platelets from the patient, her husband, their son, and healthy unrelated controls. ADP inhibited intracellular cAMP levels in platelets from the patient's husband, son and healthy unrelated controls (not shown) by approximately 80%, whereas the inhibition was only 15% in the patient's platelets (Fig. 3). In contrast to ADP, epinephrine normally inhibited cAMP accumulation in platelets from the patient as well as her husband and son. These results strongly suggest that the defect could be due to an abnormality in G_i coupling ADP receptor, $P2Y_{12}$.

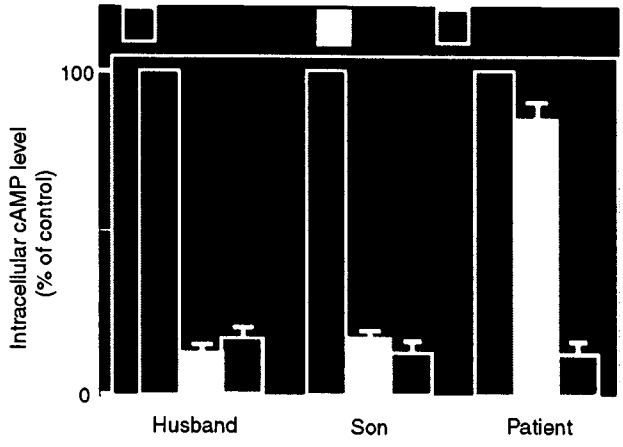

Fig. 3. Effect of ADP or epinephrine on the inhibition of PGE_1-induced cAMP accumulation in platelets. Washed platelets from patient OSP-1, husband or son were incubated with 1 μM of PGE_1 for 15 min and stimulated with 20 μM of ADP or 10 μM of epinephrine. Intracellular cAMP levels were expressed as a percent of cAMP levels in the absence of agonists. Results in OSP-1 are the mean of two experiments.

Nucleotide sequence analysis of cDNA and genomic DNA of $P2Y_{12}$

To reveal a molecular genetic defect in OSP-1, we analyzed the entire coding regions of both $P2Y_1$ and $P2Y_{12}$ cDNAs amplified from platelet mRNA by RT-PCR. A single nucleotide substitution (T → G) was identified within the translation initiation codon (ATG → AGG) in the patient's $P2Y_{12}$ cDNA (Fig. 4A). This substitution was also confirmed by reverse sequencing. No other nucleotide substitutions were detected within the coding region of either $P2Y_{12}$ or $P2Y_1$ cDNA from the patient. OSP-1 appeared homozygous for the substitution, and the substitution was not detected in 20 control subjects.

Nucleotide sequence analysis of PCR fragments from the patient's genomic DNA also suggested the homozygosity of the substitution (data not shown). To further confirm the homo-

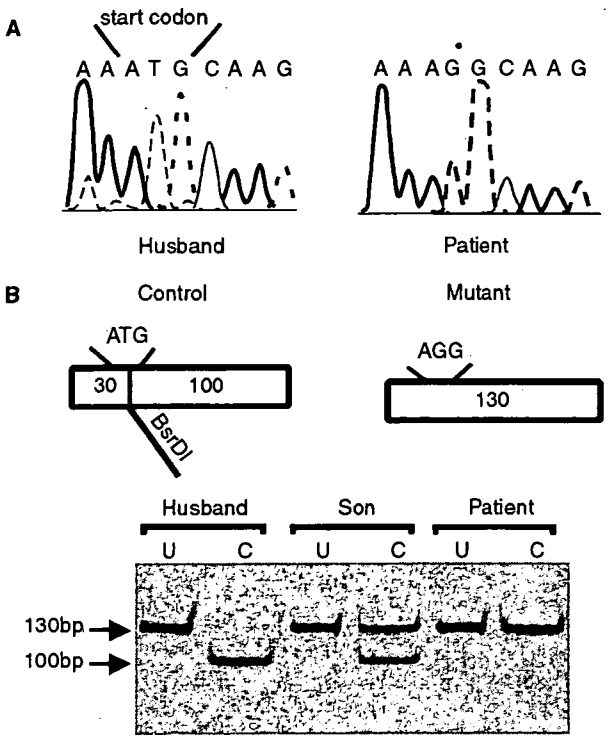

Fig. 4. Sequence analysis of $P2Y_{12}$ cDNA and restriction enzyme analysis of the $P2Y_{12}$ gene. (A) cDNA obtained by RT-PCR from platelet mRNA was analyzed by sequencing using a sense primer Y12F1. (B) PCR was performed to generate 130-bp fragments including initiation codon of $P2Y_{12}$ as described in Materials and methods. Undigested (U) or digested (C) PCR products with *BsrDI* were analyzed on a 6% polyacrylamide gel. In patient OSP-1, the T → G mutation at position 2 abolishes a *BsrDI* restriction site.

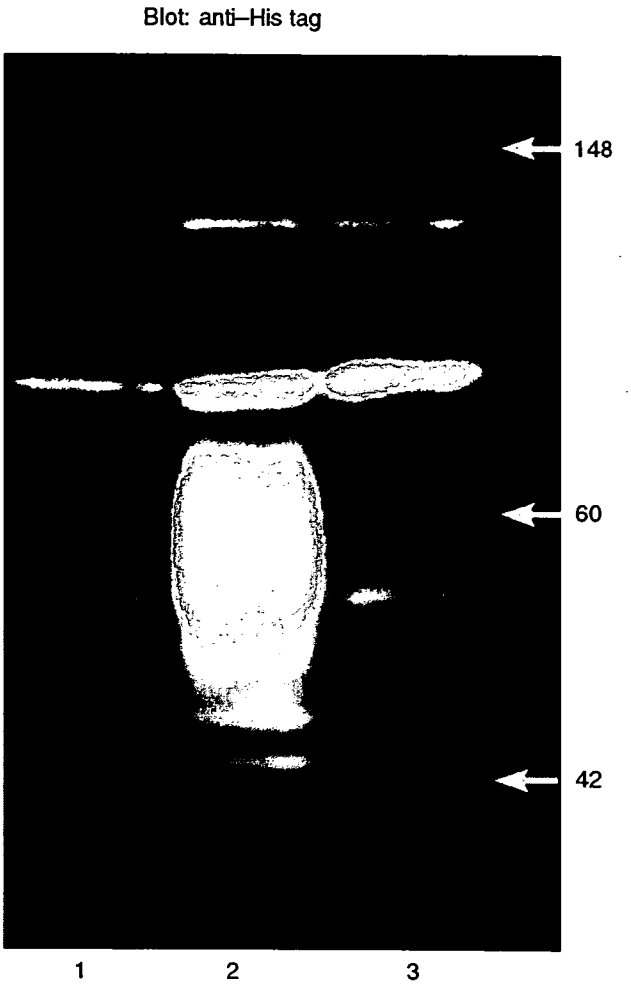

Fig. 5. Expression of $P2Y_{12}$ in HEK293 cells transfected with WT or mutant His-tag attached $P2Y_{12}$. Wild-type or mutant $P2Y_{12}$ construct was transfected into HEK293 cells using the calcium phosphate method. Transfectants were lyzed by 1% Triton X-100 PBS containing protease inhibitors 2 days after transfection. Cell lysates from mock transfectant (lane 1), cells transfected with WT $P2Y_{12}$ (lane 2) or mutant $P2Y_{12}$ (lane 3) were separated by 7.5% SDS-PAGE, and immunoblot was performed by anti-His-tag antibodies.

zygosity, allele-specific restriction enzyme analysis (ASRA) was performed. The region around the initiation codon of the $P2Y_{12}$ gene was amplified by PCR using primers BsrDI-GF and Y12R4. A restriction site for *BsrDI* would be abolished by the T → G substitution. As shown in Fig. 4B, ASRA clearly indicated that the patient and her son were homozygous and heterozygous for the substitution, respectively. These results also confirm that the substitution is inheritable.

Heterologous cell expression of WT and mutant $P2Y_{12}$

As the substitution at the translation initiation codon might induce an alternative translation starting at downstream ATGs leading to an expression of shorter form of $P2Y_{12}$, we decided to investigate effects of the substitution found in the patient on the expression of $P2Y_{12}$. Expression vectors encoding WT and mutant $P2Y_{12}$ in which His-tag was attached at the C-terminal portion of $P2Y_{12}$ were constructed as described in the Materials and methods. Wild-type or mutant $P2Y_{12}$ construct was transfected into HEK 293 cells, and then expressed proteins were analyzed 48 h after transfection in an immunoblot assay employing anti-His antibodies. As shown in Fig. 5, WT $P2Y_{12}$ protein with an apparent molecular weight of ~60 KDa was expressed in 293 cells as a His-tag-positive protein. In sharp contrast, the mutant $P2Y_{12}$-expression vector failed to express any His-tag-positive protein. These results provide strong evidence that the T → G substitution at the translation initiation codon of $P2Y_{12}$ cDNA is responsible for the $P2Y_{12}$ deficiency.

Platelet spreading on immobilized fibrinogen

As it has been well documented that release of endogenous ADP is required for full platelet spreading onto immobilized fibrinogen [23], we next analyzed the patient's platelet spreading in order to evaluate the role of $P2Y_{12}$. Control platelets adhered to fibrinogen underwent morphological changes ranging from filopodia protrusion to complete spreading, and 50.5% ± 21.3% of the adherent platelets spread ($n = 3$) (Fig. 6A). In sharp contrast, the patient's platelets showed an

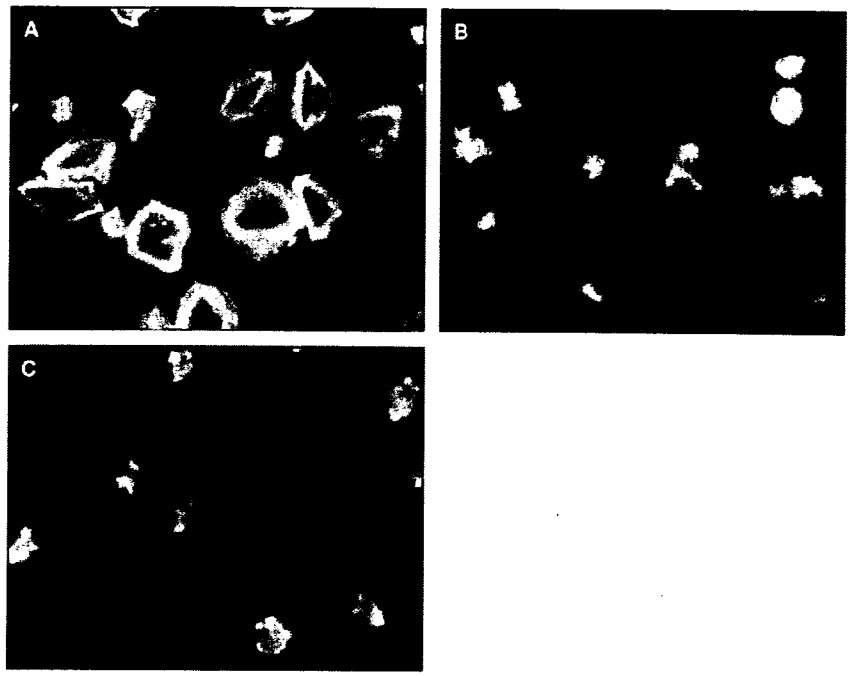

Fig. 6. Platelet spreading on immobilized fibrinogen. (A,B) Washed platelets from a control subject were applied onto fibrinogen-coated polystyrene dishes and incubated at 37 °C for 40 min without any inhibitor (A) or with 1 μM of AR-C69931MX (B). (C) Washed platelets from the patient were applied onto fibrinogen-coated polystyrene dishes and incubated at 37 °C for 40 min without any inhibitor. Adherent platelets were then fixed, permeabilized and stained with TRITC-conjugated phalloidin. Platelet morphology was analyzed by fluorescence microscopy.

impaired spreading and only 2.3% ± 1.4% of the adherent platelets spread ($n = 3$, $P < 0.001$, Fig. 6C). Similar results were obtained with control platelets in the presence of 1 μM of AR-C69931MX (6.2% ± 2.2%, $n = 3$, $P < 0.001$, Fig. 6B). In addition, 1 mM of A3P5P also markedly inhibited platelet spreading ($n = 3$, 10.1% ± 2.2%, $P < 0.001$, not shown). These results suggest that both $P2Y_{12}$ and $P2Y_1$ are necessary for platelet spreading.

Platelet-thrombus formation on immobilized collagen under flow conditions

To investigate the role of $P2Y_{12}$ in thrombus formation, we observed the real-time process of mural thrombogenesis on a type I collagen-coated surface under flow conditions with high shear rate (2000 s^{-1}) using the whole blood from OSP-1. Real-time observation revealed that thrombi formed on type I collagen were unstable. As platelet aggregates of the patient were loosely packed each other and unable to resist against high shear stress, most of the aggregates at the apex of the thrombi came off the thrombi constantly. On the other hand, most of thrombi formed by control platelets were densely packed with higher fluorescent intensity and were stable with constant growth during observation (Video 1 and 2).

As shown in Fig. 7A, the area covered with patient platelets after 7 min of flow was greater than that of control platelets (91.8% ± 0.3% vs. 82.2% ± 1.4%, $n = 3$, $P < 0.01$). However, thrombi formed by OSP-1 platelets were loosely packed, whereas thrombi were large and densely packed in controls. The overall fluorescent intensity of thrombi of OSP-1 platelets was lower than that of control platelets. Three-dimensional analysis revealed the striking difference in size and shape of individual thrombus formed after 10 min between the patient and control platelets (Fig. 7B). Thrombi formed by control platelets were large in size, clearly edged and surrounded by thrombus-free areas. On the other hand, individual thrombus formed by patient platelets was mostly small and appeared to be a thin layer of platelet aggregates. Thrombus height at the plateau phase was 10.2 ± 0.4 μm, which was less than half of controls (21.2 ± 0.4 μm).

Discussion

$P2Y_{12}$ coupled with $G\alpha_i$, primarily with $G\alpha_{i2}$, consists of 342 amino acid residues with seven transmembrane domains (TM), and its deficiency is responsible for congenital bleeding diathesis [10–16]. To date, five mutations responsible for a defect in the expression or the function of $P2Y_{12}$ in four different families have been demonstrated [10,15,16]. Patient ML possessed a mutation consisting of a two nucleotide deletion at amino acid 240 (near the N-terminal end of TM6), which would lead to a premature termination of $P2Y_{12}$ [10,14]. A two nucleotide deletions at amino acid 98 (next to the N-terminal end of TM3) and a single nucleotide deletion occurring just beyond TM3 were identified in other two families, both of which would lead to a premature termination of $P2Y_{12}$ [13,15]. However, in these reports expression studies had not been performed to show the direct association between these mutations and the $P2Y_{12}$ deficiency [10,15]. Patient AC, whose platelets expressed dysfunctional $P2Y_{12}$ with normal

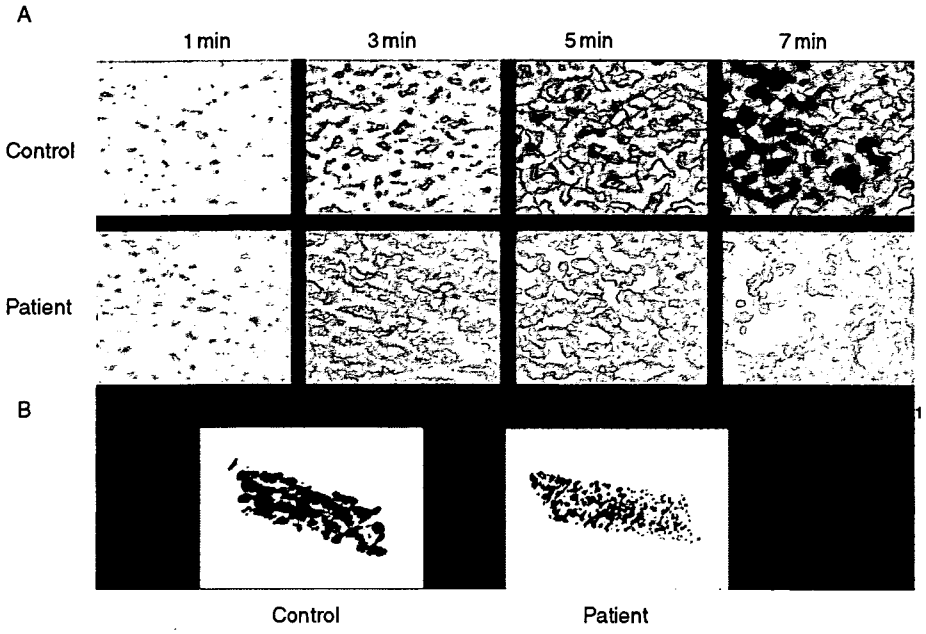

Fig. 7. Thrombus formation on immobilized collagen under flow conditions. (A) Whole blood containing mepacrine-labeled platelets obtained from the patient or control subjects was aspirated through a chamber with type I collagen-coated coverslips. Thrombi formed under a high shear rate (2000 s^{-1}) at indicated time points were observed using a microscope equipped with epifluorescent illumination and a CCD camera system. (B) Three-dimensional structure of thrombi formed after 10 min flow by platelets from the patient or a control subject was analyzed.

binding capacity of 2-methylthioadenosine 5′-diphosphate (2MeS-ADP), was compound heterozygous for Arg256 → Gln in TM6 and for Arg265 → Trp in the third extracellular loop of P2Y$_{12}$. Platelets from patient AC showed an increased platelet aggregation at high dose ADP compared with low dose ADP, suggesting the presence of residual receptor function [16]. In this study, we described a patient (OSP-1) with congenital bleeding diathesis bearing a novel homozygous mutation within the translation initiation codon (ATG → AGG) of the P2Y$_{12}$ gene. Consistent with previous studies, the aggregation of OSP-1 platelets with P2Y$_{12}$ deficiency was impaired to various agonists such as collagen, U46619, and PAR1 TRAP at low concentrations, but almost normal at high concentrations [11–14]. These findings confirmed that a critical role of P2Y$_{12}$-mediated signaling evoked by endogenous ADP in platelet aggregation induced by low concentrations of agonists. In contrast to patient AC with residual P2Y$_{12}$-mediated signaling, the impaired platelet aggregation in OSP-1 in response to ADP was neither improved even at 100 μM of ADP stimulation nor reduced by adding 1 μM of AR-C69931MX, suggesting a complete loss of the P2Y$_{12}$ function. Family study confirmed that patient OSP-1 was homozygous for the mutation, and our expression study demonstrated that the mutation is responsible for the P2Y$_{12}$ deficiency.

A number of examples of mutations in the translation initiation codons have been demonstrated in various diseases [24]. Although some cases having mutations in the initiation codons did not express any related abnormal protein, Pattern *et al.* showed an abnormal Gα_s protein possibly synthesized as a result of initiation at downstream ATGs due to a mutation at an initiation codon (ATG → GTG) in patients with Albright's hereditary osteodystrophy [24,25]. In OSP-1, we detected the T → G mutation at position +2, and our expression study denied the possibility that the substitution might induce an alternative translation at downstream ATGs leading to an expression of shorter form of P2Y$_{12}$.

As to platelet spreading onto immobilized fibrinogen, OSP-1 platelets showed the impaired platelet spreading. Similarly, A3P5P inhibited the platelet spreading. It has been well documented that release of endogenous ADP is required for full platelet spreading onto immobilized fibrinogen [23], and Obergfell *et al.* [26] have demonstrated that the platelet spreading requires sequential activation of Src and Syk in proximately to $\alpha_{IIb}\beta_3$. In contrast to the ADP-induced platelet shape change shown in OSP-1 platelets in the platelet aggregometer, our data indicated that both P2Y$_{12}$ and P2Y$_1$ were necessary for the full spreading onto immobilized fibrinogen.

Employing clopidogrel or AR-C69931 MX as an inhibitor for P2Y$_{12}$, several studies examined the role of P2Y$_{12}$ in thrombogenesis under flow conditions [27–30]. However, some discrepancy between the studies was pointed out and non-specific effects of these inhibitors were not completely ruled out [28–30]. As patient OSP-1 was deficient in P2Y$_{12}$ as shown in this study, it would be informative to examine the real-time process of thrombogenesis on a type I collagen-coated surface under a high shear rate (2000 s^{-1}) employing whole blood obtained from OSP-1. Our data demonstrated that P2Y$_{12}$-deficiency led to the loosely packed thrombus and the impaired thrombus growth with enhancing adhesion to collagen, which was consistent with the study by Remijn *et al.* [30] employing patient ML's platelets. The increase in platelet adhesion to

collagen was probably due to the impaired platelet consumption by the growing thrombi [27,30]. Moreover, our real-time observation indicated that the loosely packed aggregates were unable to resist against high shear stress, and then most of the aggregates at the apex of the thrombi came off the thrombi. In contrast, Andre *et al.* [12] did not detect significant differences in *ex vivo* thrombus volume formed over human type III collagen under a shear rate of 871 s^{-1} between $P2Y_{12}^{-/-}$ and WT mice. Although Andre *et al.* used non-anticoagulated mouse blood instead of anticoagulated blood, Roald *et al.* [27] demonstrated that clopidogrel significantly reduced the thrombus volume over type III collagen employing non-anticoagulated human blood. Loosely packed platelet thrombi with swollen non-degranulated platelets were detected following clopidogrel intake, whereas densely packed thrombi with partly fused platelets were detected before clopidogrel intake by electron microscopy [27]. Thus, it is likely that differences between human and mouse, rather than those between non-anticoagulated and anticoagulated blood, may account for the discrepancy. Nevertheless, they showed that *ex vivo* thrombi were loosely packed and that only small and unstable thrombi were formed in $P2Y_{12}^{-/-}$ mice without reaching occlusive size in mesenteric artery injury model *in vivo* [12].

Our present study has demonstrated the novel mutation responsible for the $P2Y_{12}$ deficiency and suggested that secretion of endogenous ADP and subsequent $P2Y_{12}$-mediated signaling is critical for platelet aggregation, platelet spreading, and as a consequence, for stabilization of thrombus. Mild bleeding tendency observed in patient OSP-1 further emphasizes the efficacy of $P2Y_{12}$ receptor as a therapeutic target for thrombosis.

Acknowledgements

We thank Dr Mitsuhiko Sugimoto (Nara Medical University) for his valuable advice to perform the real-time observation of thrombogenesis under flow conditions. This study was supported in part by Grant-in Aid for Scientific Research from the Ministry of Education, Science and Culture in Japan, Yamanouchi Foundation for Research on Metabolic Disorder, Tukuba, Japan, and Mitsubishi Pharma Research Foundation, Osaka, Japan.

Supplementary material

The following supplementary material is available online:

Figure S1. Perfusion study using control platelets. A real-time movie of platelets perfused over type-I collagen shows that thrombi formed by control platelets are densely packed and stable. This 5-second movie was taken at 5-minute perfusion under a high shear rate (2000 s^{-1}).

Figure S2. Perfusion study using OSP-1 platelets. A real-time movie of platelets perfused over type-I collagen shows that thrombi formed by the patient OSP-1 platelets are loosely packed and unstable. Newly formed aggregates on the top of thrombi keep on moving toward downstream and some aggregates came off the thrombi. This 5-second movie was taken at 5-minute perfusion under a high shear rate (2000 s^{-1}).

References

1 Fuster V, Badimon L, Badimon JJ, Chesebro JH. The pathogenesis of coronary artery disease and the acute coronary syndromes. *N Engl J Med* 1992; **326**: 242–50.

2 Antithrombotic Trialists' Collaboration. Collaborative meta-analysis of randomised trials of antiplatelet therapy for prevention of death, myocardial infarction, and stroke in high risk patients. *BMJ* 2002; **324**: 71–86.

3 Savage B, Almus-Jacobs F, Ruggeri ZM. Specific synergy of multiple substrate–receptor interactions in platelet thrombus formation under flow. *Cell* 1998; **94**: 657–66.

4 Tomiyama Y, Shiraga M, Shattil SJ. Platelet Membrane Proteins as Adhesion Receptors. In: Gresele P, Page C, Fuster V, Vermylen J, eds. *Platelets in thrombotic and non-thrombotic disorders pathophysiology, pharmacology and therapeutics.* Cambridge, UK: Cambridge, 2002: 80–92.

5 CAPRIE Steering Committee. A randomised, blinded, trial of clopidogrel versus aspirin in patients at risk of ischaemic events (CAPRIE). *Lancet* 1996; **348**: 1329–39.

6 Gachet C. ADP receptors of platelets and their inhibition. *Thromb Haemost* 2001; **86**: 222–32.

7 Dorsam RT, Kunapuli SP. Central role of the $P2Y_{12}$ receptor in platelet activation. *J Clin Invest* 2004; **113**: 340–5.

8 Fabre JE, Nguyen M, Latour A, Keifer JA, Audoly LP, Coffman TM, Koller BH. Decreased platelet aggregation, increased bleeding time and resistance to thromboembolism in $P2Y_1$-deficient mice. *Nat Med* 1999; **5**: 1199–202.

9 Leon C, Hechler B, Freund M, Eckly A, Vial C, Ohlmann P, Dierich A, LeMeur M, Cazenave JP, Gachet C. Defective platelet aggregation and increased resistance to thrombosis in purinergic $P2Y_1$ receptor-null mice. *J Clin Invest* 1999; **104**: 1731–7.

10 Hollopeter G, Jantzen HM, Vincent D, Li G, England L, Ramakrishnan V, Yang RB, Nurden A, Julius D, Conley PB. Identification of the platelet ADP receptor targeted by antithrombotic drugs. *Nature* 2001; **409**: 202–7.

11 Foster CJ, Prosser DM, Agans JM, Zhai Y, Smith MD, Lachowicz JE, Zhang FL, Gustafson E, Monsma Jr FJ, Wiekowski MT, Abbondanzo SJ, Cook DN, Bayne ML, Lira SA, Chintala MS. Molecular identification and characterization of the platelet ADP receptor targeted by thienopyridine antithrombotic drugs. *J Clin Invest* 2001; **107**: 1591–8.

12 Andre P, Delaney SM, LaRocca T, Vincent D, DeGuzman F, Jurek M, Koller B, Phillips DR, Conley PB. $P2Y_{12}$ regulates platelet adhesion/activation, thrombus growth, and thrombus stability in injured arteries. *J Clin Invest* 2003; **112**: 398–406.

13 Cattaneo M, Lecchi A, Randi AM, McGregor JL, Mannucci PM. Identification of a new congenital defect of platelet function characterized by severe impairment of platelet responses to adenosine diphosphate. *Blood* 1992; **80**: 2787–96.

14 Nurden P, Savi P, Heilmann E, Bihour C, Herbert JM, Maffran JP, Nurden A. An inherited bleeding disorder linked to a defective interaction between ADP and its receptor on platelets. Its influence on glycoprotein IIb-IIIa complex function. *J Clin Invest* 1995; **95**: 1612–22.

15 Conley P, Jurek M, Vincent D, Lecchi A, Cattaneo M. Unique mutations in the $P2Y_{12}$ locus of patients with previously described defects in ADP-dependent aggregation [abstract]. *Blood* 2001; **98**: 43b. Abstract 3778.

16 Cattaneo M, Zighetti ML, Lombardi R, Martinez C, Lecchi A, Conley PB, Ware J, Ruggeri ZM. Molecular bases of defective signal

transduction in the platelet P2Y$_{12}$ receptor of a patient with congenital bleeding. *Proc Natl Acad Sci USA* 2003; **100**: 1978–83.

17 Shiraga M, Tomiyama Y, Honda S, Suzuki H, Kosugi S, Tadokoro S, Kanakura Y, Tanoue K, Kurata Y, Matsuzawa Y. Involvement of Na^+/Ca^{2+} exchanger in inside-out signaling through the platelet integrin $\alpha_{IIb}\beta_3$. *Blood* 1998; **92**: 3710–20.

18 Tomiyama Y, Tsubakio T, Piotrowicz RS, Kurata Y, Loftus JC, Kunicki TJ. The Arg-Gly-Asp (RGD) recognition site of platelet glycoprotein IIb-IIIa on nonactivated platelets is accessible to high-affinity macromolecules. *Blood* 1992; **79**: 2303–12.

19 Honda S, Tomiyama Y, Aoki T, Shiraga M, Kurata Y, Seki J, Matsuzawa Y. Association between ligand-induced conformational changes of integrin $\alpha_{IIb}\beta_3$ and $\alpha_{IIb}\beta_3$-mediated intracellular Ca^{2+} signaling. *Blood* 1998; **92**: 3675–83.

20 Kato H, Honda S, Yoshida H, Kashiwagi H, Shiraga M, Honma N, Kurata K, Tomiyama Y. SHPS-1 negatively regulates integrin $\alpha_{IIb}\beta_3$ function through CD47 without disturbing FAK phosphorylation. *J Thromb Haemost* 2005; **3**: 763–74.

21 Tsuji S, Sugimoto M, Miyata S, Kuwahara M, Kinoshita S, Yoshioka A. Real-time analysis of mural thrombus formation in various platelet aggregation disorders: distinct shear-dependent roles of platelet receptors and adhesive proteins under flow. *Blood* 1999; **94**: 968–75.

22 Honda S, Tomiyama Y, Shiraga M, Tadokoro S, Takamatsu J, Saito H, Kurata Y, Matsuzawa Y. A two-amino acid insertion in the Cys146-Cys167 loop of the α_{IIb} subunit is associated with a variant of Glanzmann thrombasthenia. Critical role of Asp163 in ligand binding. *J Clin Invest* 1998; **102**: 1183–92.

23 Haimovich B, Lipfert L, Brugge JS, Shattil SJ. Tyrosine phosphorylation and cytoskeletal reorganization in platelets are triggered by interaction of integrin receptors with their immobilized ligands. *J Biol Chem* 1993; **268**: 15868–77.

24 Cooper D. Human gene mutations affecting RNA processing and translation. *Ann Med* 1993; **25**: 11–7.

25 Patten J, Johns D, Valle D, Eil C, Gruppuso PA, Steele G, Smallwood PM, Levine MA. Mutation in the gene encoding the stimulatory G protein of adenylate cyclase in Albright's hereditary osteodystrophy. *N Engl J Med* 1990; **322**: 1412–9.

26 Obergfell A, Eto K, Mocsai A, Buensuceso C, Moores SL, Brugge JS, Lowell CA, Shattil SJ. Coordinate interactions of Csk, Src, and Syk kinases with αIIbβ3 initiate integrin signaling to the cytoskeleton. *J Cell Biol* 2002; **157**: 265–75.

27 Roald HE, Barstad RM, Kierulf P, Skjorten F, Dickinson JP, Kieffer G, Sakariassen KS. Clopidogrel - a platelet inhibitor which inhibits thrombogenesis in non-anticoagulated human blood independently of the blood flow conditions. *Thromb Haemost* 1994; **71**: 655–62.

28 Turner NA, Moake JL, McIntire LV. Blockade of adenosine diphosphate receptors P2Y$_{12}$ and P2Y$_1$ is required to inhibit platelet aggregation in whole blood under flow. *Blood* 2001; **98**: 3340–5.

29 Goto S, Tamura N, Handa S. Effects of adenosine 5′-diphosphate (ADP) receptor blockade on platelet aggregation under flow. *Blood* 2002; **99**: 4644–5.

30 Remijn JA, Wu YP, Jeninga EH, IJsseldiik MJ, van Willigen G, de Groot PG, Sixma JJ, Nurden AT, Nurden P. Role of ADP receptor P2Y$_{12}$ in platelet adhesion and thrombus formation in flowing blood. *Arterioscler Thromb Vasc Biol* 2002; **22**: 686–91.

Measurement of ADAMTS13 activity and inhibitors

Toshiyuki Miyata, Koichi Kokame and Fumiaki Banno

Purpose of review
Acquired or congenital deficiency in the plasma von Willebrand factor-cleaving protease ADAMTS13 causes life-threatening thrombotic thrombocytopenic purpura. This condition is characterized primarily by thrombocytopenia and microangiopathic hemolytic anemia, accompanied by variable degrees of neurologic dysfunction, renal failure, and fever. Measurement of ADAMTS13 activity is important in the diagnosis of microangiopathies such as thrombotic thrombocytopenic purpura. This review introduces both established and emerging assays for ADAMTS13 activity, focusing on their impact on clinical practice.
Recent findings
Previously established assays are useful screening methods to identify suspected thrombotic thrombocytopenic purpura. Novel assays measuring ADAMTS13 activity using either recombinant peptides or synthetic substrates directly measure the activity quantitatively. These assays can also detect neutralizing autoantibodies in the plasma of patients with acquired ADAMTS13 deficiency. Although ADAMTS13 in control subjects exhibits a broad variation in activity, ranging from 30 to 200%, significant decreases in ADAMTS13 activity have been observed in several physiologic and pathologic conditions. A portion of thrombotic thrombocytopenic purpura patients, however, did not display severe ADAMTS13 deficiency, suggesting that as-yet-unidentified environmental or genetic factors may contribute to the etiology of thrombotic thrombocytopenic purpura.
Summary
New assays measuring ADAMTS13 activity will contribute significantly to the accurate diagnosis of microangiopathies, ultimately leading to improved clinical treatment of these diseases. These assays may also help to clarify the role of ADAMTS13 activity in additional thrombotic disorders, including disseminated intravascular coagulation, stroke, and myocardial infarction.

Keywords
ADAMTS13, microangiopathy, thrombotic thrombocytopenic purpura

Curr Opin Hematol 12:384–389.

National Cardiovascular Center Research Institute, Osaka, Japan

Supported in part by grants-in-aid from the Ministry of Health, Labor, and Welfare of Japan and the Ministry of Education, Culture, Sports, Science, and Technology of Japan.

Correspondence to Toshiyuki Miyata, PhD, National Cardiovascular Center Research Institute, 5-7-1 Fujishirodai, Suita, Osaka 565-8565, Japan
Tel: +81 6 6833 5012, ext: 2512, 8123; fax: +81 6 6835 1176;
e-mail: miyata@ri.ncvc.go.jp

Current Opinion in Hematology 2005, 12:384–389

Abbreviations

TSP-1	thrombospondin type 1
TTP	thrombotic thrombocytopenic purpura
ULVWF	ultralarge von Willebrand factor
VWF	von Willebrand factor

1065-6251

Introduction

Thrombotic thrombocytopenic purpura (TTP) is characterized by thrombocytopenia and microangiopathic hemolytic anemia, accompanied by variable penetrance of neurologic dysfunction, renal failure, and fever [1,2,3•,4••,5••]. TTP leads to the development of systemic microvascular thrombi of platelets, largely resulting from the accumulation of ultralarge von Willebrand factor (ULVWF) multimers in plasma. The accumulation of ULVWF multimers is caused by congenital or acquired deficiency in a von Willebrand factor (VWF)-cleaving protease, ADAMTS13, a metalloprotease of the ADAMTS family (a disintegrinlike and metalloprotease with thrombospondin type I motifs) [6•–9•]. ADAMTS13 was purified and cloned by several groups in 2001 [10–15]. As the basic and clinical studies on TTP and ADAMTS13 have greatly advanced since this discovery, this review focuses on the available assays measuring ADAMTS13 activity. We also discuss the sensitivity and specificity of ADAMTS13 activity assessment in the diagnosis of TTP.

Pathogenesis of thrombotic thrombocytopenic purpura

VWF, a substrate of ADAMTS13, is a multimeric protein important for platelet adhesion to subendothelial connective tissue. In vascular endothelial cells, the primary site of VWF production, VWF dimers are initially formed through formation of a disulfide bond near the C-termini. The prosequences of the VWF dimer are cleaved, followed by formation of ULVWF multimers by generation of a disulfide bond near the N-termini. ULVWF multimers are either stored in Weibel–Palade bodies or secreted into the plasma. Under normal circumstances, ULVWF multimers are unfolded by high shear stress in the circulation, making internal sites available for proteolysis by ADAMTS13, which specifically cleaves the peptide bond between Y1605 and M1606 in the A2 domain of VWF. Cleavage depolymerizes the ULVWF complexes into smaller multimers. Functional deficiency of ADAMTS13, resulting from either genetic mutations [16•] or inhibitory autoantibody production, leads to the accumulation of ULVWF multimers in plasma. These multimers promote intravascular thrombi of platelets, resulting in platelet

consumption and hemolysis. After the formation of microvascular thrombi in the kidney or brain, patients may suffer renal failure or neurologic dysfunction [1,2,3•,4••,5••].

Recent progress of ADAMTS13

The domain structure of ADAMTS13 shares similarities with other ADAMTS proteases, but is most divergent among this family [13] that contains 19 members in humans [17•]. ADAMTS13 is synthesized predominantly in the liver [12–15], although expression has been observed in other tissues and cell types, including platelets [18•]. In sequence, the 1427 amino acid precursor contains a signal peptide, a short propeptide, a metalloprotease domain, a disintegrinlike domain, a thrombospondin type 1 (TSP-1) repeat, a Cys-rich domain, a spacer domain, seven additional TSP-1 repeats, and two CUB domains [12–15]. CUB domains are named for complement components C1r/C1s, urinary epidermal growth factor, and bone morphogenic protein-1, each of which has one or more CUB domains [2]. Although propeptides are generally necessary to preserve the latency of metalloproteases, the ADAMTS13 propeptide is not required for enzyme latency [19]. The metalloprotease domain is necessary, but not sufficient, for VWF cleavage, indicating the requirement for other domains in VWF cleavage [20,21]. A single nucleotide polymorphism within the Cys-rich domain, encoding a P475S mutation, is found in the Japanese population at an allelic frequency of approximately 5% [22]. This mutant exhibits low, but significant, VWF-cleaving activity, suggesting a role for the Cys-rich domain in proteolysis. Although this polymorphism is also found in the Chinese population at a lower frequency, it has not been identified in the white population [16•,23,24]. The spacer domain is indispensable for VWF cleaving activity. Truncation mutants lacking the spacer domain lose activity in both static and flow conditions [20,21,25•]. Inhibitory autoantibodies against ADAMTS13 in patients with acquired TTP are directed against epitopes in the Cys-rich and spacer domains [20,26••,27]. In addition, a truncated ADAMTS13 resulting from insertion of the retroviruslike element has been identified in a number of mouse strains [28••]. This truncated form, lacking the C-terminal two TSP-1 motifs and two CUB domains, exhibits the same activity levels as the full-length form. Although the exact cleavage sites have not been determined, both thrombin and plasmin can cleave ADAMTS13, resulting in the loss of activity [29••].

Extensive study has elucidated the mechanisms underlying the interaction of ADAMTS13 with VWF. VWF has three A-type domains; ADAMTS13 cleaves the central A2 domain. Homology modeling estimates that a scissile peptide bond exists inside the A2 domain [30]. The VWF A1 and A3 domains are binding sites for platelet GPIba and collagen respectively. Although the A1 domain inhibits cleavage of the A2 domain by ADAMTS13, this inhibition is reversed on interaction of the A1 domain with platelet GPIba or heparin [31••]. A single nucleotide polymorphism in the VWF A2 domain encoding a Y1584C mutation is found in the population of the United Kingdom with an allelic frequency of about 0.5%. This mutant VWF protein demonstrated an increased susceptibility for ADAMTS13 proteolysis [32,33].

Assays of ADAMTS13 activity

Five methods are widely used to assay ADAMTS13 activity [4••,34•]: multimer analysis by SDS-agarose gel electrophoresis [35], analysis of degraded VWF by SDS–polyacrylamide gel electrophoresis [36], two-site immunoradiometric analysis [37], residual collagen binding analysis [38], and residual ristocetin cofactor activity analysis [39].

Pioneering work using a recombinant A1-A2-A3 VWF fragment expressed in Drosophila cells has recently been described for measuring ADAMTS13 activity [40]. This assay requires denatured cleavage conditions and uses Western blotting to detect the products.

Investigators demonstrated that ULVWF multimers newly released from endothelial cells are anchored to the surfaces of endothelial cells in a P-selectin-dependent manner [41•] and form long stringlike structures to which fluorescence-labeled platelets adhere [42]. Based on these finding, the cleavage of endothelial-derived ULVWF multimers under flow was used to examine ADAMTS13 activity [43•]. After the cleavage of these strings on endothelial cells under flow by ADAMTS13, the numbers of ULVWF strings were quantified as a measure of enzyme activity.

Evaluation of these methods

A multicenter comparison has been organized to evaluate these assays [44]. ADAMTS13 activity was determined in 30 plasma samples, with activities ranging from less than 3 to more than 100%, from patients with congenital or acquired TTP and other unrelated conditions by four different analyses: the multimer analysis by SDS–agarose gel electrophoresis, the two-site immunoradiometric analysis, the residual collagen binding analysis, and the residual ristocetin cofactor activity analysis. All assays identified plasma samples with severe ADAMTS13 deficiencies (<5%) and those with strong inhibitory activity, with some exceptions of results observed using the collagen binding assay. Plasma samples with normal to moderately reduced activity exhibited less concordant results.

An additional international collaborative study evaluated these four methods, as well as two additional methods [45•]: a quantitative immunoblotting assay using a recombinant VWF A1-A2-A3 fragment [40] and a cleavage assay using endothelial cell-derived ULVWF stringlike structures with attached platelets under flow [43]. In this study, measurement of six plasma samples with 0%, 10%, 20%,

40%, 80%, and 100% of ADAMTS13 activity indicated that the most consistent and reliable assays were the multimer analysis by SDS–agarose gel electrophoresis, the residual collagen binding analysis, and the residual ristocetin cofactor activity analysis.

New assays using recombinant or synthetic substrates

The assays described here use multimeric forms of VWF as substrates that require denaturing conditions, such as urea, for cleavage. Most of these assays measure the residual activity of VWF multimers, likely resulting in a reduced sensitivity for the quantification of ADAMTS13 activity. Therefore, more accurate and simpler methods are desired. Recently, novel ADAMTS13 assays have been developed using both recombinant and synthetic substrates. These high-throughput methods are rapid and do not require denaturing conditions or protease-free purified VWF substrates.

An assay using the minimal VWF region required to serve as a specific substrate has been attempted [46•]. The substrate peptide, designated GST-VWF73-H, consists of a 73-amino acid sequence spanning residues D1596 to R1668 of the VWF A2 domain, designated VWF73. This sequence is flanked by an N-terminal glutathione S-transferase and six C-terminal His sequences. This assay does not require a denaturing condition for cleavage, but necessitates Western blotting for detection.

To avoid the use of Western blotting, a fluorogenic peptide (FRETS-VWF73) was synthesized [47••]. FRETS-VWF73 contains the core VWF73 peptide, in which the Q1599 residue at the P7 position of the scissile bond was converted to a 2,3-diaminopropionic residue (A2pr) modified with a 2-(N-methyl amino)benzoyl group (Nma). The N1610 residue at the P5# position was converted to A2pr modified with a 2,4-dinitrophenyl group (Dnp; Fig. 1). When the Nma group is exited at 340 nm, fluorescence resonance energy is transferred to the neighboring quencher, Dnp. After cleavage of the bond between Y1605 and M1606 by ADAMTS13, the quenching of fluorescence resulting from the energy transfer does not occur, allowing the emission of fluorescence at 440 nm by Nma. Thus, incubation of FRETS-VWF73 with plasma samples containing ADAMTS13 resulted in a quantitative increase in fluorescence. Neither thrombin nor plasmin increased fluorescence of FRETS-VWF73. The analysis can be completed within 1 hour using a 96-well format and commercial plate readers. FRETS-VWF73 is now commercially available from the Peptide Institute, Inc. (Minoh, Japan).

A novel enzyme immunoassay-based method using recombinant GST-VWF73-H has also been described [48•]. In this assay, GST-VWF73-H was captured onto anti-GST precoated microtiter plates and, after incubation with plasma samples, the remaining amount of intact GST-VWF73-H is detected with an anti-His epitope antibody.

Figure 1. Structure of the synthetic fluorogenic ADAMTS13 substrate FRETS-VWF73

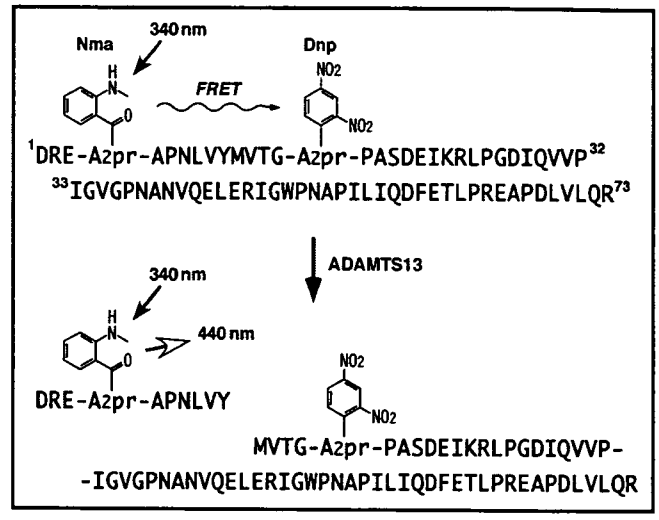

FRET, fluorescence resonance energy transfer; Nma, 2-(N-methyl amino) benzoyl group; Dnp, 2,4-dinitrophenyl group; A2pr, 2,3-diaminopropionic residue.

The recombinant A2 domain, flanked with six N-terminal His residues and a C-terminal Tag-100 sequence, was also used for an ADAMTS13 activity assay [49,50•]. The A2 peptide, captured on a Ni^{2+}-coated microtiter plate, was incubated with plasma samples. After washing, the amount of A2 peptide remaining in the well was detected with a monoclonal antibody against the Tag-100 sequence.

Detection of autoantibodies

All the assay methods described here are useful to detect ADAMTS13 autoantibodies in plasma of patients with acquired TTP. An inhibitor assay is generally carried out using mixtures of heat-inactivated plasma from patients and normal plasma at 1:1 dilution or several dilutions. The amount of activity inhibited by 1 mL of the patient's plasma was then estimated; thus, 1 U of inhibitor neutralizes the activity in 1 mL of normal human plasma [51]. Alternatively, the protease activity in the mixture was expressed as a percentage of that in control plasma. For the detection of autoantibodies against ADAMTS13, an ELISA kit is now commercially available from Technoclone GmbH (Vienna, Austria).

Precaution for measurement of ADAMTS13 activity in plasma

To measure ADAMTS13 activity, blood is normally collected into tubes containing sodium citrate as an anticoagulant. As ADAMTS13 is a metalloprotease, inclusion of EDTA completely inhibits enzyme activity. A high

concentration of hemoglobin (more than 2 g/L) has also been reported to inhibit ADAMTS13 cleavage [52]. Plasma concentrations of VWF also potentially affect ADAMTS13 activity; the VWF present in plasma samples would competitively inhibit substrate cleavage. As the plasma concentrations of VWF vary under a subset of pathologic conditions, coexisting pathologies may complicate ADAMTS13 activity assay results.

Factors influencing ADAMTS13 activity

Decreases in ADAMTS13 activity have been reported in liver cirrhosis, chronic uremia, acute inflammatory states, idiopathic thrombocytopenic purpura, disseminated intravascular coagulation, and systemic lupus erythematosus [53,54]. In addition, decreased activity has been observed in the postoperative state, the neonatal period, pregnancy, and aging [47••,53,55,56]. Infusion of the vasopressin analog desmopressin or endotoxin also transiently decreased ADAMTS13 activity [57,58•,59•]. ADAMTS13 activities in control samples exhibit a broad range of values, ranging from 30 to 200% of the mean activity [37,38,47••,51,53,60]. Mild decreases in ADAMTS13 activity in newborns were reported in one study, whereas others have observed normal levels [53,61,62]. Plasma ADAMTS13 activity exhibits a negative correlation with VWF protein and activity levels [53,58•]. Women typically exhibit higher ADAMTS13 activity levels than men [47••].

Sensitivity and specificity of decreased ADAMTS13 activity for diagnosis of thrombotic thrombocytopenic purpura

Severe deficiency in ADAMTS13 activity specifically distinguishes TTP from other thrombotic microangiopathies [63•,64•]. Increasing evidence, however, has questioned the sensitivity of decreased ADAMTS13 activity for diagnosis of TTP and the specificity of ADAMTS13 deficiency as a means to discriminate TTP from other microangiopathies. A population of TTP patients does not exhibit severe ADAMTS13 deficiency [40,53,60,65–67,68•]. These exceptions to the classic correlation between phenotype and genotype in TTP patients have to consider when the ADAMTS13 activity is used for a diagnostic use. These observations may suggest that as-yet-unidentified environmental or genetic factors contribute to the etiology of TTP [5••].

Limitation of assays

Hopefully these new assay methods will be used in clinical practice. Many of these methods, however, still have limitations; with one exception: All these assays use static conditions that do not resemble the physiologic milieu. Each still necessitates a couple of hours to complete and requires special equipment, such as a plate reader. These requirements limit practical use of these assays at a well-equipped institution. All these assays use pooled plasma as a standard, despite the wide range of ADAMTS13 activities among individual plasma samples. Recombinant ADAMTS13 should therefore be used as the standard. For bedside practice in a wide range of clinical settings, simpler and apparatus-free methods are in demand.

Measurements of ADAMTS13 antigen level

ADAMTS13 ELISA kits designed to monitor plasma antigen levels of ADAMTS13 have recently become available from several companies, including Technoclone GmbH and Mitsubishi Kagaku Iatron, Inc. (Tokyo, Japan).

Conclusion

In addition to established assays for ADAMTS13 activity, novel assays using recombinant or synthetic substrates have recently been developed. Although time will be needed to evaluate these analyses, such high-throughput methods will contribute significantly to the accurate diagnosis of microangiopathies, ultimately leading to improved treatment of these diseases. These assays may also help clarify the role of ADAMTS13 in thrombotic disorders, including disseminated intravascular coagulation, stroke, and myocardial infarction. Although severe deficiency in ADAMTS13 activity is an established cause of TTP, recent clinical studies have indicated a more complicated relation of ADAMTS13 deficiency with TTP. Intensive studies of patients with microangiopathies are needed to clarify this discrepancy.

Acknowledgements

The authors thank Dr Masanori Matsumoto and Dr Yoshihiro Fujimura at Nara Medical University for their continuous collaborative work.

References and recommended reading

Papers of particular interest, published within the annual period of review, have been highlighted as:

- • of special interest
- •• of outstanding interest

1 Moake JL. Thrombotic microangiopathies. N Engl J Med 2002; 347:589–600.

2 George JN, Sadler JE, Lämmle B. Platelets: thrombotic thrombocytopenic purpura. Hematology (Am Soc Hematol Educ Program) 2002:315–334.

3 • Lämmle B, George JN. Thrombotic thrombocytopenic purpura: advances in pathophysiology, diagnosis, and treatment—introduction. Semin Hematol 2004; 41:1–3.
This article is an introductory remark of special issue of Seminars in Hematology.

4 •• Sadler JE, Moake JL, Miyata T, et al. Recent advances in thrombotic thrombocytopenic purpura. Hematology (Am Soc Hematol Educ Program) 2004: 407–423.
This review focused on idiopathic TTP, new ADAMTS13 assays and clinical applications, and the clinical course and long-term outcomes of TTP.

5 •• Levy GG, Motto DG, Ginsburg D. ADAMTS13 turns 3. Blood 2005. Prepublished online.
This review summarizes the progress of TTP and ADAMTS13 analyses since the cloning of the VWF-cleaving protease cDNA in 2001.

6 • Furlan M. Proteolytic cleavage of von Willebrand factor by ADAMTS-13 prevents uninvited clumping of blood platelets. J Thromb Haemost 2004; 2: 1505–1509.
This is a historical sketch on ADAMTS13 by Dr. Furlan, devoted to TTP research.

7 • Tsai HM. A journey from sickle cell anemia to ADAMTS13. J Thromb Haemost 2004; 2:1510–1514.
This is a historical sketch on ADAMTS13 by Dr. Tsai, devoted to TTP research.

8 Moake JL. Defective processing of unusually large von Willebrand factor multimers and thrombotic thrombocytopenic purpura. J Thromb Haemost 2004; 2:1515–1521.
This is a historical sketch on ADAMTS13 by Dr. Moake, who discovered ULVWF multimers in TTP patients' plasma.

9 Soejima K, Nakagaki T. Interplay between ADAMTS13 and von Willebrand factor in inherited and acquired thrombotic microangiopathies. Semin Hematol 2005; 42:56–62.
This review deals with the advances in TTP research after the cloning of ADAMTS13 cDNA in 2001.

10 Gerritsen HE, Robles R, Lämmle B, et al. Partial amino acid sequence of purified von Willebrand factor-cleaving protease. Blood 2001; 98:1654–1661.

11 Fujikawa K, Suzuki H, McMullen B, et al. Purification of human von Willebrand factor-cleaving protease and its identification as a new member of the metalloproteinase family. Blood 2001; 98:1662–1666.

12 Soejima K, Mimura N, Hirashima M, et al. A novel human metalloprotease synthesized in the liver and secreted into the blood: possibly, the von Willebrand factor-cleaving protease? J Biochem (Tokyo) 2001; 130:475–480.

13 Zheng X, Chung D, Takayama TK, et al. Structure of von Willebrand factor-cleaving protease (ADAMTS13), a metalloprotease involved in thrombotic thrombocytopenic purpura. J Biol Chem 2001; 276:41059–41063.

14 Levy GG, Nichols WC, Lian EC, et al. Mutations in a member of the ADAMTS gene family cause thrombotic thrombocytopenic purpura. Nature 2001; 413: 488–494.

15 Plaimauer B, Zimmermann K, Volkel D, et al. Cloning, expression, and functional characterization of the von Willebrand factor-cleaving protease (ADAMTS13). Blood 2002; 100:3626–3632.

16 Kokame K, Miyata T. Genetic defects leading to hereditary thrombotic thrombocytopenic purpura. Semin Hematol 2004; 41:34–40.
This review summarizes the genetic defects and polymorphisms in the ADAMTS13 gene that have been identified in patients with TTP.

17 Nicholson AC, Malik SB, Logsdon JM Jr, et al. Functional evolution of ADAMTS genes: evidence from analyses of phylogeny and gene organization. BMC Evol Biol 2005; 5:11.
This article describes the phylogenetic relationship between all human ADAMTS genes, including a comparison with invertebrate and chordate ADAMTS homologues.

18 Suzuki M, Murata M, Matsubara Y, et al. Detection of von Willebrand factor-cleaving protease (ADAMTS-13) in human platelets. Biochem Biophys Res Commun 2004; 313:212–216.
The authors identified ADAMTS13 expression in human platelets.

19 Majerus EM, Zheng X, Tuley EA, et al. Cleavage of the ADAMTS13 propeptide is not required for protease activity. J Biol Chem 2003; 278:46643–46648.

20 Soejima K, Matsumoto M, Kokame K, et al. ADAMTS-13 cysteine-rich/spacer domains are functionally essential for von Willebrand factor cleavage. Blood 2003; 102:3232–3237.

21 Zheng X, Nishio K, Majerus EM, et al. Cleavage of von Willebrand factor requires the spacer domain of the metalloprotease ADAMTS13. J Biol Chem 2003; 278:30136–30141.

22 Kokame K, Matsumoto M, Soejima K, et al. Mutations and common polymorphisms in ADAMTS13 gene responsible for von Willebrand factor-cleaving protease activity. Proc Natl Acad Sci U S A 2002; 99:11902–11907.

23 Ruan C, Dai L, Su J, et al. The frequency of P475S polymorphism in von Willebrand factor-cleaving protease in the Chinese population and its relevance to arterial thrombotic disorders. Thromb Haemost 2004; 91:1257–1258.

24 Bongers TN, De Maat MPM, Dippel DWJ, et al. Absence of Pro475Ser polymorphisms in ADAMTS13 in Caucasians. J Thromb Haemost 2005; 3. Prepublished online.

25 Tao Z, Wang Y, Choi H, et al. Cleavage of ultra-large multimers of von Willebrand factor by C-terminal truncated mutants of ADAMTS-13 under flow. Blood 2005. Prepublished online.
The authors investigated the ADAMTS13 activity of C-terminal-truncated mutants under flow conditions.

26 Klaus C, Plaimauer B, Studt JD, et al. Epitope mapping of ADAMTS13 autoantibodies in acquired thrombotic thrombocytopenic purpura. Blood 2004; 103:4514–4519.
The authors examined the epitopes recognized by inhibitory autoantibodies specific for ADAMTS13 and identified Cys-rich and spacer domains as the major targeted epitopes. CUB domains and first TSP-1 domain also demonstrated some reactivity.

27 Luken BM, Turenhout EA, Hulstein JJ, et al. The spacer domain of ADAMTS13 contains a major binding site for antibodies in patients with thrombotic thrombocytopenic purpura. Thromb Haemost 2005; 93:267–274.

28 Banno F, Kaminaka K, Soejima K, et al. Identification of strain-specific variants of mouse Adamts13 gene encoding von Willebrand factor-cleaving protease. J Biol Chem 2004; 279:30896–30903.
In mice, two types of ADAMTS13 mutants were present in a strain-specific manner. These mutations are caused by the insertion of an intracisternal A particle retrotransposon introducing a premature stop codon.

29 Crawley JT, Lam JK, Rance JB, et al. Proteolytic inactivation of ADAMTS13 by thrombin and plasmin. Blood 2005; 105:1085–1093.
The authors found that ADAMTS13 is degraded by thrombin and plasmin in vitro, resulting in the loss of VWF cleaving activity.

30 Sutherland JJ, O'Brien LA, Lillicrap D, et al. Molecular modeling of the von Willebrand factor A2 domain and the effects of associated type 2A von Willebrand disease mutations. J Mol Model (Online) 2004; 10:259–270.

31 Nishio K, Anderson PJ, Zheng XL, et al. Binding of platelet glycoprotein Ibα to von Willebrand factor domain A1 stimulates the cleavage of the adjacent domain A2 by ADAMTS13. Proc Natl Acad Sci U S A 2004; 101:10578–10583.
The authors reported a Y1584C mutation, 22 residues N-terminal to the ADAMTS13 scissile site, within the A2 domain of VWF. Carriers of this mutation demonstrated increased susceptibility of VWF to proteolysis by ADAMTS13.

32 Bowen DJ, Collins PW. An amino acid polymorphism in von Willebrand factor correlates with increased susceptibility to proteolysis by ADAMTS13. Blood 2004; 103:941–947.

33 Bowen DJ, Collins PW, Lester W, et al. The prevalence of the cysteine 1584 variant of von Willebrand factor is increased in type 1 von Willebrand disease: co-segregation with increased susceptibility to ADAMTS13 proteolysis but not clinical phenotype. Br J Haematol 2005; 128:830–836.

34 Veyradier A, Girma JP. Assays of ADAMTS-13 activity. Semin Hematol 2004; 41:41–47.
This review introduced five ADAMTS13 assay methods.

35 Furlan M, Robles R, Lämmle B. Partial purification and characterization of a protease from human plasma cleaving von Willebrand factor to fragments produced by in vivo proteolysis. Blood 1996; 87:4223–4234.

36 Tsai HM. Physiologic cleavage of von Willebrand factor by a plasma protease is dependent on its conformation and requires calcium ion. Blood 1996; 87:4235–4244.

37 Obert B, Tout H, Veyradier A, et al. Estimation of the von Willebrand factor-cleaving protease in plasma using monoclonal antibodies to vWF. Thromb Haemost 1999; 82:1382–1385.

38 Gerritsen HE, Turecek PL, Schwarz HP, et al. Assay of von Willebrand factor (vWF)-cleaving protease based on decreased collagen binding affinity of degraded vWF: a tool for the diagnosis of thrombotic thrombocytopenic purpura (TTP). Thromb Haemost 1999; 82:1386–1389.

39 Bohm M, Vigh T, Scharrer I. Evaluation and clinical application of a new method for measuring activity of von Willebrand factor-cleaving metalloprotease (ADAMTS13). Ann Hematol 2002; 81:430–435.

40 Remuzzi G, Galbusera M, Noris M, et al. von Willebrand factor cleaving protease (ADAMTS13) is deficient in recurrent and familial thrombotic thrombocytopenic purpura and hemolytic uremic syndrome. Blood 2002; 100:778–785.

41 Padilla A, Moake JL, Bernardo A, et al. P-selectin anchors newly released ultralarge von Willebrand factor multimers to the endothelial cell surface. Blood 2004; 103:2150–2156.
The authors found that ULVWF multimers are anchored to the surface of endothelial cells through P-selectin after stimulation with histamine.

42 Dong JF, Moake JL, Nolasco L, et al. ADAMTS-13 rapidly cleaves newly secreted ultralarge von Willebrand factor multimers on the endothelial surface under flowing conditions. Blood 2002; 100:4033–4039.

43 Dong JF, Whitelock J, Bernardo A, et al. Variations among normal individuals in the cleavage of endothelial-derived ultra-large von Willebrand factor under flow. J Thromb Haemost 2004; 2:1460–1466.
The authors measured ADAMTS13 activity using platelet-decorated ULVWF strings bound to endothelial cells under flow conditions.

44 Studt JD, Bohm M, Budde U, et al. Measurement of von Willebrand factor-cleaving protease (ADAMTS-13) activity in plasma: a multicenter comparison of different assay methods. J Thromb Haemost 2003; 1:1882–1887.

45 Tripodi A, Chantarangkul V, Bohm M, et al. Measurement of von Willebrand factor cleaving protease (ADAMTS-13): results of an international collaborative study involving 11 methods testing the same set of coded plasmas. J Thromb Haemost 2004; 2:1601–1609.
This international multicenter study evaluated 11 methods measuring ADAMTS13 activity.

46 Kokame K, Matsumoto M, Fujimura Y, et al. VWF73, a region from D1596 to
• R1668 of von Willebrand factor, provides a minimal substrate for ADAMTS-13. Blood 2004; 103:607–612.
Using recombinant techniques, the authors identified the minimal substrate region for ADAMTS13 cleavage, composed of 73 amino acid residues from the A2 domain of VWF.

47 Kokame K, Nobe Y, Kokubo Y, et al. FRETS-VWF73, a fluorogenic substrate
•• for ADAMTS13 assay. Br J Haemost 2005; 129:93–100.
FRETS-VWF73 was developed as a fluorogenic substrate for an ADAMTS13 activity assay using fluorescence resonance energy transfer.

48 Zhou W, Tsai HM. An enzyme immunoassay of ADAMTS13 distinguishes
• patients with thrombotic thrombocytopenic purpura from normal individuals and carriers of ADAMTS13 mutations. Thromb Haemost 2004; 91:806–811.
Recombinant GST-VWF73-H was used for an ADAMTS13 activity assay.

49 Cruz MA, Whitelock J, Dong JF. Evaluation of ADAMTS-13 activity in plasma using recombinant von Willebrand Factor A2 domain polypeptide as substrate. Thromb Haemost 2003; 90:1204–1209.

50 Whitelock JL, Nolasco L, Bernardo A, et al. ADAMTS-13 activity in plasma is
• rapidly measured by a new ELISA method that uses recombinant VWF-A2 domain as substrate. J Thromb Haemost 2004; 2:485–491.
A recombinant A2 domain of VWF was used for an ADAMTS13 activity assay.

51 Furlan M, Robles R, Galbusera M, et al. von Willebrand factor-cleaving protease in thrombotic thrombocytopenic purpura and the hemolytic–uremic syndrome. N Engl J Med 1998; 339:1578–1584.

52 Studt JD, Hovinga JA, Antoine G, et al. Fatal congenital thrombotic thrombo-
• cytopenic purpura with apparent ADAMTS13 inhibitor: in vitro inhibition of ADAMTS13 activity by hemoglobin. Blood 2005; 105:542–544.
The authors observed that extremely high concentrations of hemoglobin interfere with ADAMTS13 activity.

53 Mannucci PM, Canciani MT, Forza I, et al. Changes in health and disease of the metalloprotease that cleaves von Willebrand factor. Blood 2001; 98: 2730–2735.

54 Moore JC, Hayward CP, Warkentin TE, et al. Decreased von Willebrand factor protease activity associated with thrombocytopenic disorders. Blood 2001; 98:1842–1846.

55 Lattuada A, Rossi E, Calzarossa C, et al. Mild to moderate reduction of a von Willebrand factor cleaving protease (ADAMTS-13) in pregnant women with HELLP microangiopathic syndrome. Haematologica 2003; 88:1029–1034.

56 Sanchez–Luceros A, Farias CE, Amaral MM, et al. von Willebrand factor-cleaving protease (ADAMTS13) activity in normal non-pregnant women, pregnant and post-delivery women. Thromb Haemost 2004; 92:1320–1326.

57 Reiter RA, Knobl P, Varadi K, et al. Changes in von Willebrand factor-cleaving protease (ADAMTS13) activity after infusion of desmopressin. Blood 2003; 101:946–948.

58 Reiter RA, Varadi K, Turecek PL, et al. Changes in ADAMTS13 (von-
• Willebrand-factor-cleaving protease) activity after induced release of von Willebrand factor during acute systemic inflammation. Thromb Haemost 2005; 93:554–558.
The authors observed that systemic inflammation induced by intravenous infusion of endotoxin decreased after 4 to 24 hours and returned to normal after 7 days.

59 Mannucci PM, Capoferri C, Canciani MT. Plasma levels of von Willebrand
• factor regulate ADAMTS-13, its major cleaving protease. Br J Haematol 2004; 126:213–218.
The authors discovered that individuals with blood group O have higher ADAMTS13 activity than non-O group individuals. In addition, infusion of desmopressin decreased ADAMTS13 activity.

60 Veyradier A, Obert B, Houllier A, et al. Specific von Willebrand factor-cleaving protease in thrombotic microangiopathies: a study of 111 cases. Blood 2001; 98:1765–1772.

61 Tsai HM, Sarode R, Downes KA. Ultralarge von Willebrand factor multimers and normal ADAMTS13 activity in the umbilical cord blood. Thromb Res 2002; 108:121–125.

62 Schmugge M, Dunn MS, Amankwah KS, et al. The activity of the von Willebrand factor cleaving protease ADAMTS-13 in newborn infants. J Thromb Haemost 2004; 2:228–233.

63 Matsumoto M, Yagi H, Ishizashi H, et al. The Japanese experience with throm-
• botic thrombocytopenic purpura-hemolytic uremic syndrome. Semin Hematol 2004; 41:68–74.
A total of 290 Japanese patients with TTP-HUS were reported.

64 Hovinga JA, Studt JD, Alberio L, et al. von Willebrand factor-cleaving protease
• (ADAMTS-13) activity determination in the diagnosis of thrombotic microangiopathies: the Swiss experience. Semin Hematol 2004; 41:75–82.
A total of 396 consecutive patients referred to Dr. Lämmle's laboratory for diagnosis purposes were summarized.

65 Bianchi V, Robles R, Alberio L, et al. Von Willebrand factor-cleaving protease (ADAMTS13) in thrombocytopenic disorders: a severely deficient activity is specific for thrombotic thrombocytopenic purpura. Blood 2002; 100:710–713.

66 Vesely SK, George JN, Lämmle B, et al. ADAMTS13 activity in thrombotic thrombocytopenic purpura–hemolytic uremic syndrome: relation to presenting features and clinical outcomes in a prospective cohort of 142 patients. Blood 2003; 102:60–68.

67 Snider CE, Moore JC, Warkentin TE, et al. Dissociation between the level of von Willebrand factor-cleaving protease activity and disease in a patient with congenital thrombotic thrombocytopenic purpura. Am J Hematol 2004; 77:387–390.

68 Peyvandi F, Ferrari S, Lavoretano S, et al. von Willebrand factor cleaving pro-
• tease (ADAMTS-13) and ADAMTS-13 neutralizing autoantibodies in 100 patients with thrombotic thrombocytopenic purpura. Br J Haematol 2004; 127:433–439.
The authors investigated 100 patients with TTP, discovering that 48% patients exhibited severely reduced ADAMTS13 activity and 28% showed normal levels.

THE JOURNAL OF BIOLOGICAL CHEMISTRY VOL. 281, NO. 2, pp. 850–857, January 13, 2006

Zinc and Calcium Ions Cooperatively Modulate ADAMTS13 Activity*

Received for publication, April 26, 2005, and in revised form, October 7, 2005 Published, JBC Papers in Press, November 11, 2005, DOI 10.1074/jbc.M504540200

Patricia J. Anderson‡, Koichi Kokame§, and J. Evan Sadler‡1

From the ‡Howard Hughes Medical Institute, Department of Medicine, Washington University School of Medicine, St. Louis, Missouri 63110 and the §National Cardiovascular Center Research Institute, Osaka 565-8565, Japan

ADAMTS13 is a metalloproteinase that cleaves von Willebrand factor (VWF) multimers. The metal ion dependence of ADAMTS13 activity was examined with multimeric VWF and a fluorescent peptide substrate based on Asp^{1596}–Arg^{1668} of the VWF A2 domain, FRETS-VWF73. ADAMTS13 activity in citrate-anticoagulated plasma was enhanced ~ 2-fold by zinc ions, ~ 3-fold by calcium ions, and ~ 6-fold by both ions, suggesting cooperative activation. Cleavage of VWF by recombinant ADAMTS13 was activated up to ~ 200-fold by zinc ions ($K_{D\ app}$ ~ 0.5 ~ M), calcium ions ($K_{D\ app}$ ~ 4.8 ~ M), and barium ions ($K_{D\ app}$ ~ 1.7 mM). Barium ions stimulated ADAMTS13 activity in citrated plasma but not in citrate-free plasma. Therefore, the stimulation by barium ions of ADAMTS13 in citrated plasma appears to reflect the release of chelated calcium and zinc ions from complexes with citrate. At optimal zinc and calcium concentrations, ADAMTS13 cleaved VWF with a $K_{m\ app}$ of 3.7 ~ 1.4 ~ g/ml (~ 15 nM for VWF subunits), which is comparable with the plasma VWF concentration of 5–10 ~ g/ml. ADAMTS13 could cleave ~ 14% of VWF pretreated with guanidine HCl, suggesting that this substrate is heterogeneous in susceptibility to proteolysis. ADAMTS13 cleaved FRETS-VWF73 with a $K_{m\ app}$ of 3.2 ~ 1.1 ~ M, consistent with an ~ 200-fold decrease in affinity compared with VWF. ADAMTS13 cleaved VWF and FRETS-VWF73 with roughly comparable catalytic efficiency of 55 ~ M^{-1} min^{-1} and 18 ~ M^{-1} min^{-1}, respectively. The striking preference of ADAMTS13 for VWF suggests that substrate recognition depends on structural features or exosites on multimeric VWF that are missing from FRETS-VWF73.

The von Willebrand factor (VWF)[2] cleaving proteinase ADAMTS13 is a member of the ADAMTS (a disintegrin and metalloproteinase with thrombospondin repeats") family (1–3). Since the identification of ADAMTS13, evidence has increased concerning the association of severe ADAMTS13 deficiency with the disease thrombotic thrombocytopenic purpura (TTP) (4–6). TTP is characterized by disseminated microvascular thrombi containing platelets and multimers of VWF, which is a plasma protein that mediates platelet adhesion by tethering platelets to the extracellular matrix (7, 8). In the absence of ADAMTS13 activity, ultra-large multimers of VWF accumulate, causing persistent intravascular platelet aggregation and TTP. Congenital TTP, or Upshaw-Schulman syndrome, is caused by compound heterozygous or homozygous mutations in the ADAMTS13 gene (2, 9, 10). Acquired idiopathic TTP usually affects adults and is caused predominantly by autoimmune responses to ADAMTS13 (6). The mortality rate is ~ 90% if untreated; however, plasma exchange therapy has reduced this rate to ~ 20% (11–13).

Many proteinases of the ADAMTS family are involved in extracellular matrix remodeling, angiogenesis, and development, where they typically cleave large multimeric proteins (14, 15). ADAMTS13 regulates the size of plasma VWF multimers by proteolytic cleavage at Tyr^{1605}–Met^{1606} within the A2 domain of VWF subunits (4, 16). ADAMTS proteinases contain a reprolysin-like zinc metalloproteinase domain, a disintegrin domain, a cysteine-rich and spacer region, several thrombospondin type 1 repeats, and variable C termini, which in ADAMTS13 includes two CUB domains (named for the first identified proteins containing this motif, complement C1r/C1s, Uegf, and Bmp1) (17). The metalloproteinase domain of ADAMTS13 has a putative zinc ion catalytic site (^{224}HEXXHXXGXXHD^{235}), one predicted calcium ion-binding site coordinated by residues Glu^{83}, Asp^{173}, Cys^{281}, and Asp^{284}, and a conserved Met^{249} that supports the active site zinc ion in a "Met turn"; these features identify ADAMTS13 as a member of the "metzincin" family (1, 18, 19). The metzincins, which include the homologous matrix metalloproteinases and ADAMs (a disintegrin and metalloproteinase), achieve optimal activity with both zinc and calcium ions (18–22).

The role of divalent metal ions in ADAMTS13 activity is not fully understood. Previous studies of ADAMTS13 activity reported that a combination of barium and calcium ions was optimal for cleavage of VWF (4, 5, 23). The addition of zinc ions has yielded inconsistent results; some studies found no effect, whereas others found that zinc ions restored the activity of EDTA-treated ADAMTS13 (4, 23). In addition, interactions of ADAMTS13 with VWF depend upon ionic strength and pH, but optimal conditions vary considerably among several reports. When assayed at pH 8.0, ADAMTS13 activity was greatest under conditions of low ionic strength (4). Other studies have demonstrated proteolysis of VWF by ADAMTS13 at low ionic strength (I ~ 75 mM) in the absence of added metal ions (6).

The previous studies of ADAMTS13 proteolysis of VWF have established that interactions between the enzyme and substrate are dependent upon metal ions and electrostatic interactions. However, these studies have generally employed reaction conditions unlike those prevailing in vivo. Therefore, the properties of ADAMTS13 were investigated under physiological conditions of pH and ionic strength. The enzyme was found to be activated by calcium and zinc ions at concentrations typical of plasma. Additionally, the $K_{m\ app}$ for VWF was within the range of plasma VWF concentrations, but the $K_{m\ app}$ for a synthetic peptide based on the sequence of cleavage site within the VWF A2-domain was ~ 210-fold higher. This difference indicates that structural features or

* This work was supported in part by American Heart Association National Scientist Development Award 0530110N (to P. J. A.) and by National Institutes of Health Grant HL72917. The costs of publication of this article were defrayed in part by the payment of page charges. This article must therefore be hereby marked "advertisement" in accordance with 18 U.S.C. Section 1734 solely to indicate this fact.

[1] To whom correspondence should be addressed: Howard Hughes Medical Institute, WA University School of Medicine, 660 S. Euclid, Box 8022, St. Louis, MO 63110. Tel.: 314-362-9029; Fax: 314-454-3012; E-mail: esadler@im.wustl.edu.

[2] The abbreviations used are: VWF, von Willebrand factor; FFR-CK, Phe-Phe-Arg-CH_2Cl; FPR-CK, D-Phe-Pro-Arg-CH_2Cl; TTP, thrombotic thrombocytopenic purpura.

exosites within the native multimeric VWF molecule are required for efficient substrate recognition by ADAMTS13.

EXPERIMENTAL PROCEDURES

Materials—Aliquots of normal human plasma (American Red Cross, St. Louis, MO) were stored at • 20 °C until use. One unit of ADAMTS13 activity was defined as the activity in 1 ml of pooled normal human plasma. The concentration of purified human plasma VWF (Laboratoire Français du Fractionnement et des Biotechnologies, Lille, France, generously provided by Claudine Mazurier) in phosphate-buffered saline was determined by absorbance at 280 nm with an absorption coefficient of 1.0 mg ml^{-1} cm^{-1} and correction for light scattering at 340 nm as described (24).

Expression of Recombinant ADAMTS13—A cDNA encoding ADAMTS13 with a C-terminal V5-His tag (1, 25) was cloned into the tetracycline-inducible vector pcDNA4/TO (Invitrogen) at the EcoRI site to yield plasmid p4TO-ADAMTS13. TRex 293 cells (Invitrogen) were transfected with p4TO-ADAMTS13 (1 • g) using Lipofectamine 2000 (Invitrogen). Stable cell lines were maintained in Dulbecco's modified Eagle's medium containing 10% tetracycline-approved fetal bovine serum (Clontech or Invitrogen), 300 • g/ml zeocin, 5 • g/ml blasticidin, 2 mM glutamine, 5 units/ml penicillin, and 5 • g/ml streptomycin. Protein expression was initiated in 70–80% confluent roller bottles with 1 • g/ml tetracycline in Freestyle serum-free media (Invitrogen). The media were centrifuged and filtered, and proteinase inhibitors were added (0.1 • M D-Phe-Pro-Arg-CH_2Cl (FPR-CK), 0.1 • M Phe-Phe-Arg-CH_2Cl (FFR-CK), 144 • M phenylmethylsulfonyl fluoride. The media were concentrated by ultrafiltration on YM30 membranes (Millipore, Inc.) and dialyzed into an appropriate assay buffer. The concentration of recombinant ADAMTS13 was determined by standardization of Western blots with the V5-tagged Positope protein (Invitrogen) as described (25). The concentration of plasma and recombinant ADAMTS13 also was determined with the ImuBIND ADAMTS13 enzyme-linked immunosorbent assay kit (American Diagnostica, Inc.). The concentrations of plasma ADAMTS13 (0.86–0.96 • g/ml) were comparable with those estimated previously (1 • g/ml) (25). Compared with plasma ADAMTS13 (defined as 100%), the specific activity of recombinant ADAMTS13 was 64% in concentrated conditioned medium and 109% after purification to homogeneity, when assayed with FRETS-VWF73 as described below.[3]

ADAMTS13 Assays—Cleavage of VWF by ADAMTS13 was assessed by Western blotting of the 350-kDa dimer of C-terminal VWF subunit fragments (5, 6). Prior to addition, VWF was preincubated for 30 min at 37 °C in 5 mM Tris-HCl, pH 7.6, 150 mM NaCl, 1.2 M guanidine HCl. The reaction mixtures contained plasma (0.6 nM) or recombinant ADAMTS13 with various metal ion concentrations in 50 mM Hepes, pH 7.4, 50 mM NaCl, in the absence or presence of 10 mM EDTA. Similarly, recombinant ADAMTS13 activity (1 nM) was assessed in mixtures of increasing concentrations of metal ions in 50 mM Hepes, pH 7.4, 150 mM NaCl, and 1 mg/ml bovine serum albumin. Metal ion stock solutions (50 mM) were prepared in distilled water. Some metal ions required the addition of small amounts of HCl for solubility, specifically $ZnCl_2$. All reported metal ion concentrations represent the total concentration added to reactions. In complete reactions containing buffer, substrate, and plasma, Zn^{2+} was • 2 • M and Ca^{2+} was • 250 • M as determined by inductively coupled plasma spectroscopy (Mayo Clinic, Rochester, MN).

Effects of sodium ions on plasma ADAMTS13 were determined in reaction buffer containing 50 mM Hepes, pH 7.4, 0.25 mM $ZnCl_2$, 5 mM $CaCl_2$, containing either 150 mM NaCl or 150 mM choline chloride ((2-hydroxyethyl)trimethylammonium chloride), and the effects of ionic strength on plasma ADAMTS13 activity were determined by varying the concentration of NaCl in reaction buffer. The effects of guanidine HCl and urea on the cleavage of VWF were studied by varying the concentration of each chaotropic agent in 50 mM Hepes, pH 7.4, 150 mM NaCl. The reactions were preincubated at 37 °C for 10 min prior to the addition of VWF to a final concentration of 20 • g/ml or 2 • g/ml, followed by incubation at 37 °C for 1 h.

The reactions were quenched by the addition of sample loading buffer (62.5 mM Tris, pH 6.8, 1% SDS, 0.01% bromphenol blue, 5% glycerol (final concentrations)) and analyzed by SDS-PAGE on 4% or 5% gels (Invitrogen or Bio-Rad, respectively). The proteins were transferred to polyvinylidene difluoride membranes by electroblotting, and the 350-kDa product was detected by Western blotting with a 1:2500 dilution of horseradish peroxidase-conjugated rabbit anti-human VWF (DAKO, Carpinteria, CA) (26).

The observed product band densities were quantitated from scanned films using NIH Image 1.61 (rsb.info.nih.gov/nih-image/) or by chemifluorescence detected by a STORM Imager and integration of the peaks using ImageQuantTL (Amersham Biosciences). The reaction rates were calculated from the change in band density (• D_{obs}/h). The activity with added metal ions was expressed as a ratio to the activity without added metal ions and analyzed by nonlinear least squares fitting of the quadratic binding equation, with the maximal change in fold activation (• FA_{max}) and apparent dissociation constant ($K_{D\,app}$) as the fitted parameters (27). The stoichiometric factor (n) and concentration of ADAMTS13 were fixed at 1.0 and 1 nM, respectively.

Barium Ion Effects on Citrated and Noncitrated Plasma—Plasma samples were collected from healthy volunteer donors according to a protocol approved by the institutional review board of Washington University School of Medicine. Noncitrated plasma was obtained by collection into 75 • M FPR-CK, 75 • M FFR-CK, 75 • M hirudin (Sigma), and 32 • g/ml corn trypsin inhibitor (Hematologic Technologies, Inc.) (final concentrations) (28). The whole blood was centrifuged at 2000 rpm in a Sorvall 6000 for 15 min, and the recovered plasma was inhibited further by adding an additional 75 • M FPR-CK, 75 • M FFR-CK, and 32 • g/ml corn trypsin inhibitor. VWF was predenatured in 5 mM Hepes, pH 8.0, 1.23 M guanidine HCl, for 30 min at 37 °C. ADAMTS13 (0.6 nM) from citrated or noncitrated plasma was incubated with predenatured VWF (2 • g/ml) in the absence or presence of varying concentrations of $BaCl_2$ in 5 mM Hepes, pH 8.0, at 37 °C for 1 h. Effects of barium ions on 30 nM recombinant ADAMTS13 were assessed in 50 mM Hepes, pH 7.4, 150 mM NaCl, and 1 mg/ml bovine serum albumin. The reactions were quenched by the addition of 50 mM EDTA, pH 8.0, and sample loading buffer and analyzed by gel electrophoresis and Western blotting as described above. The activation of recombinant ADAMTS13 by barium ions was calculated and expressed as a ratio to the activity in the absence of added metal ions, and the data were fitted to the quadratic binding equation as described above for calcium and zinc ions. The stoichiometric factor (n) and concentration of recombinant ADAMTS13 were fixed at 1 and 30 nM, respectively.

Kinetics of VWF Cleavage—The reactions were performed with varying concentrations of VWF with plasma ADAMTS13 (0.6 nM) in assay buffer at 37 °C. The densities of the 350-kDa VWF product band were quantitated as described for metal ion-dependent reactions, and the cleavage rates were calculated as the change in product band density per hour (• D_{obs}/h). The rates of product generation as a function of VWF concentration were fit to the Michaelis-Menten equation to determine

[3] P. J. Anderson and W. Gao, unpublished observations.

the apparent Michaelis constant ($K_{m\,app}$) and maximal observed density (• $D_{obs\,max}$).

Progress curve analysis of VWF proteolysis was determined under first order reaction conditions where the [VWF] was • 0.5 • $K_{m\,app}$. The reactions contained 2 • g/ml VWF and 0.6 nM plasma ADAMTS13, in assay buffer at 37 °C. The 350-kDa VWF product band was detected by chemifluorescence. The area of the product band as a percentage of the total area from each lane as a function of time was calculated by integration of peaks using ImageQuantTL software (Amersham Biosciences). The percentage of area was multiplied by the concentration of substrate in the reaction to determine the concentration of the 350-kDa band. The progress curve of the changes in the 350-kDa VWF product band as a function of time was fit to Equation 1 to obtain the apparent first order rate constant (k_{obs}) and the maximum product generated ($[VWF]_{max}$), where k_{obs} • $E•k_{cat}/K_m$(29).

$$•VWF•_t • •VWF•_{max}•1 • e^{• k_{obst}•} \quad (1)$$

Kinetics of FRETS-VWF73 Cleavage—A peptide containing the cleavage site of ADAMTS13, consisting of Asp^{1596}–Arg^{1668} of VWF, was synthesized by the Peptide Institute (Osaka, Japan). Two amino acids flanking the cleavage site (Gln^{1599} and Asn^{1610}) were substituted with 2,3-diamino-propionic acid modified with 2-(methylamino)benzoyl and 2,4-dinitrophenol, respectively, as fluorescence resonance energy transfer donor and quencher pairs (30). Fluorescence intensities were measured with a PerkinElmer LS55 using a plate reader accessory in white 96-well plates. Increases in fluorescence intensities (F_{obs} • F_o • • F) were recorded with time using an excitation wavelength of 340 nm (5-nm band pass) and an emission wavelength of 450 nm (5-nm band pass). Various concentrations of substrate were incubated with 0.17 nM plasma ADAMTS13 in assay buffer. FRETS-VWF73 (2 • M) was cleaved to completion (17.5 h) to establish the relationship between product concentration and fluorescence intensity (• F). The observed velocities (• F/min) as a function of substrate concentration were fit to the Michaelis-Menten equation to obtain the maximum velocity (V_{max}) and the $K_{m\,app}$. Nonlinear least squares analyses were performed with Scientist software (Micromath).

Cleavage of 2 • M FRETS-VWF73 by 0.3 nM recombinant ADAMTS13 as a function of calcium and zinc ion concentration was assayed similarly in 50 mM Hepes, pH 7.4, 150 mM NaCl, and 1 mg/ml bovine serum albumin, except the instrument used was a PerkinElmer Victor^{2}V plate reader with 340-nm 25-nm bandwidth excitation filter, and 450-nm 10-nm bandwidth emission filter. The errors in the fitted parameters are reported as • 2 S.D.

RESULTS

Metal Ion Dependence of ADAMTS13 Activity—Previous studies of ADAMTS13 demonstrated that barium and calcium ions enhanced the rate of proteolysis of VWF (4), but these studies employed conditions of pH 8.0 and barium ion concentration (10 mM) that do not occur in vivo. Therefore, the metal ion activation of ADAMTS13 from both plasma and recombinant sources was re-evaluated under more physiological conditions. The interactions of metal ions with plasma ADAMTS13 were characterized by analyzing the changes in the density of the 350-kDa VWF cleavage product by Western blotting. In contrast to previous results (4), increasing concentrations of $BaCl_2$ (up to 5 mM) had little effect on the activity of ADAMTS13 at pH 7.4 (Fig. 1). Similarly, $Mg(SO_4)$ and $Cu(SO_4)$ had little effect on the activity of ADAMTS13 at pH 7.4. Increasing concentrations of $CoCl_2$, $Mn(SO_4)$, and $Ni(SO_4)$ inhibited ADAMTS13 activity. Calcium ions enhanced the activity by at least • 3-fold (up to 5 mM). Zinc ions enhanced the activity by at least

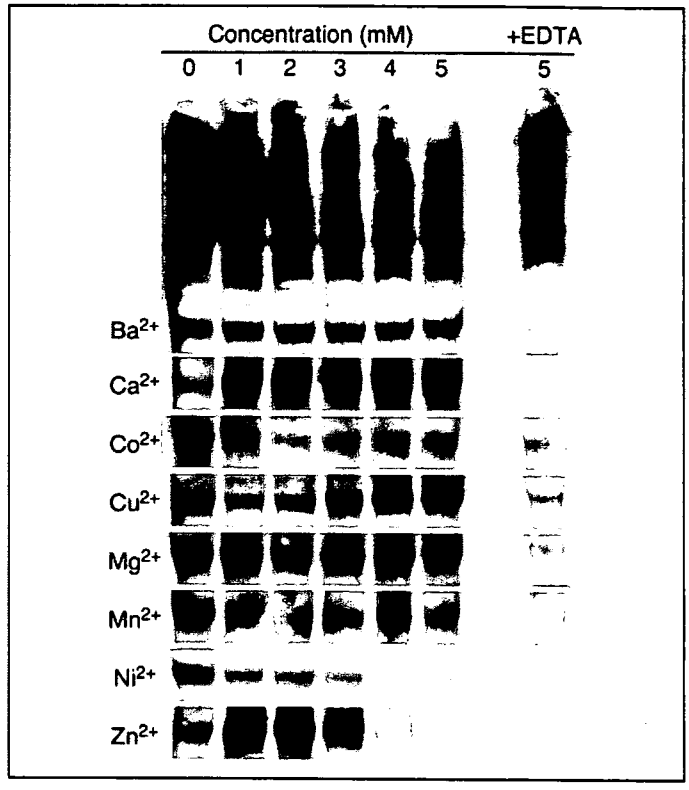

FIGURE 1. **Effects of various divalent metal ions on ADAMTS13 activity at pH 7.4.** ADAMTS13 cleavage of VWF was assessed in the absence or presence of increasing concentrations (up to 5 mM) of $BaCl_2$, $CaCl_2$, $CoCl_2$, $CuSO_4$, $MgSO_4$, $MnCl_2$, $NiSO_4$, and $ZnCl_2$. The control assays were performed with 5 mM added metal ion and 10 mM EDTA. The 350-kDa VWF product was detected by gel electrophoresis and Western blotting. The results are representative of at least three experiments.

• 2-fold (at 1 mM) (Fig. 1). ADAMTS13 activity was undetectable at concentrations of zinc ions above 3 mM, possibly because of inhibition of the enzyme by Zn(OH)$^+$ (31). Approximately 50% of the susceptible VWF was cleaved in this experiment at the optimal concentrations of $CaCl_2$ or $ZnCl_2$, and the extent of activation by these ions is underestimated slightly because of decreases in substrate concentration during the reaction. Nevertheless, the results indicate that low concentrations of zinc or calcium ions enhance the cleavage of VWF by ADAMTS13.

To determine the optimal concentration of zinc ions for plasma ADAMTS13 activity, zinc ion concentrations were varied below 250 • M (Fig. 2A). Increasing concentrations of $ZnCl_2$ enhanced the activity of ADAMTS13 by • 2-fold. (Fig. 2, A and C). The addition of 5 mM $CaCl_2$ in the presence of increasing concentrations of $ZnCl_2$ further enhanced the activity of ADAMTS13 by • 6-fold (Fig. 2, B and C). The • 6-fold increased activation demonstrated ADAMTS13 proteolysis of VWF to be dependent on both zinc and calcium ions and suggested a cooperative role of the two divalent cations.

Partial unfolding of VWF by chaotropic agents such as urea or guanidine HCl is required for rapid cleavage by ADAMTS13 in the absence of fluid shear stress (4–6, 23). To determine the effects of zinc and calcium ions on the proteolysis of VWF under these conditions, VWF was pretreated in varying concentrations of guanidine HCl or urea and then diluted 10-fold into reactions containing ADAMTS13. In the presence of zinc and calcium ions, the optimal concentration of guanidine HCl was between 1.0 and 1.25 M guanidine HCl (initial concentrations) for maximal substrate proteolysis (data not shown), which is similar to previous results (5). In contrast, preincubation of VWF in up to 2 M urea did not accelerate cleavage by ADAMTS13 (data not shown). These results suggest that distinct VWF structures are produced upon incu-

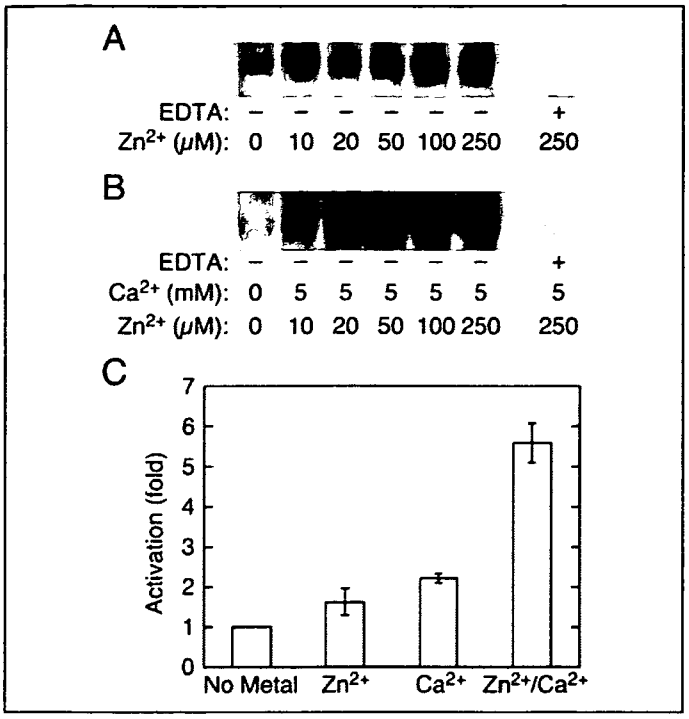

FIGURE 2. **Activation of ADAMTS13 by zinc and calcium ions.** ADAMTS13 cleavage of plasma VWF was assessed with increasing concentrations of $ZnCl_2$ (• M) in the absence (A) or presence (B) of 5 mM $CaCl_2$ without (•) or with (•) 10 mM EDTA. The 350-kDa VWF product was detected by gel electrophoresis and Western blotting. C, the activation (fold) of ADAMTS13 by 250 • M $ZnCl_2$, 5 mM $CaCl_2$, or both metal ions was determined by densitometric analysis of the Western blots in A and B and in Fig. 1 (for calcium ions alone). The error bars represent • 2 S.D. for the activation (fold) obtained for three concentrations of the varied metal that achieved the greatest activation.

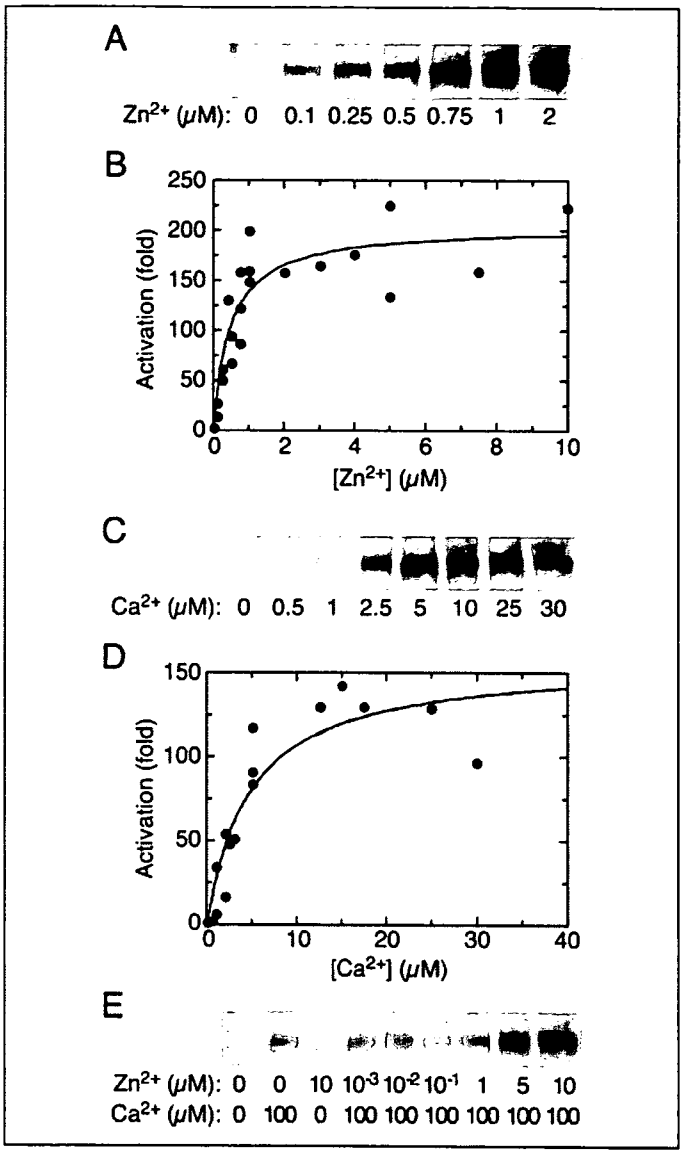

FIGURE 3. **VWF cleavage by recombinant ADAMTS13 and metal ions.** The assays contained recombinant ADAMTS13 (1 nM in A and C and 30 nM in E) and the indicated concentrations of zinc ions (A), or calcium ions (C), or both (E). The 350-kDa VWF cleavage product was detected by gel electrophoresis and Western blotting. The activation (fold) of ADAMTS13 as a function of zinc (B) or calcium (D) ion concentration was determined by chemifluorescence analysis of Western blots from several experiments including those of A and C. The lines represent the least squares fit of the quadratic binding equation to the data using the parameters described in the text.

bation with guanidine HCl or urea because the state induced by guanidine HCl persists after dilution, whereas that induced by urea does not.

The assays using citrated plasma as a source of ADAMTS13 activity typically contain • 1 mM citrate (final concentration) (4, 32). Citrate chelates a variety of divalent metal ions and could distort the apparent metal dependence of ADAMTS13 by buffering the concentration of zinc and calcium ions. Therefore, the observed effects of these cations on plasma ADAMTS13 were reassessed with recombinant ADAMTS13, which was free of citrate and other metal ion chelators (Fig. 3). Increasing concentrations of zinc ions enhanced the activity of recombinant ADAMTS13 by • 200-fold, with a $K_{D\ app}$ of 0.5 • 0.3 • M. Similarly, increasing concentrations of calcium ions enhanced the activity of recombinant ADAMTS13 by • 160-fold, with a $K_{D\ app}$ of 4.8 • 3.0 • M. The addition of zinc ions to reactions containing near saturating calcium ions (100 • M) further increased ADAMTS13 activity (Fig. 3E). These results indicate a cooperative role for calcium and zinc ions in supporting ADAMTS13 activity.

Effects of Barium Ions on ADAMTS13 Activity—Plasma ADAMTS13 activity is enhanced by the addition of barium ions, when reactions are performed using citrate anticoagulated plasma in low ionic strength buffer at pH 8.0 (4). However, little or no rate enhancement by barium ions was observed at I • 75 mM and pH 7.4 (Fig. 1), and the ability of citrate to buffer divalent metal ions suggested that the reported barium ion effects might not accurately reflect the properties of ADAMTS13. Therefore, the effect of barium ions was determined using plasma samples that were anticoagulated with sodium citrate or with nonchelating inhibitors (FPR-CK, FFR-CK, hirudin, and corn trypsin inhibitor), and reactions were performed in at low ionic strength (I • 2.5–22.5 mM) such that the citrate concentration was either 1 or 0 mM (Fig. 4A). In the presence of citrate, ADAMTS13 activity was enhanced • 2-fold by increasing concentrations of barium ions. In the absence of sodium citrate, however, ADAMTS13 activity was not affected by barium ions. Chelation of zinc and calcium ions by citrate also inhibited recombinant ADAMTS13 (Fig. 4B), supporting the conclusion that anticoagulation of plasma by citrate inhibits ADAMTS13.

To avoid the confounding effects of zinc and calcium ions in plasma, activation by barium ions was investigated using recombinant ADAMTS13. Barium ions supported ADAMTS13 activity comparable with that achieved by calcium ions, but with a $K_{D\ app}$ value of 1.7 • 0.8 mM (Figs. 3D and 4C) that is • 350-fold higher than observed for calcium ions (Fig. 3D).

Effects of Ionic Strength and Sodium Ions on ADAMTS13 Activity—In reactions containing plasma VWF and urea denaturant, ADAMTS13 in citrated plasma is markedly inhibited by increasing ionic strength and is almost inactive in 150 mM NaCl (4). In vivo, however, ADAMTS13 must

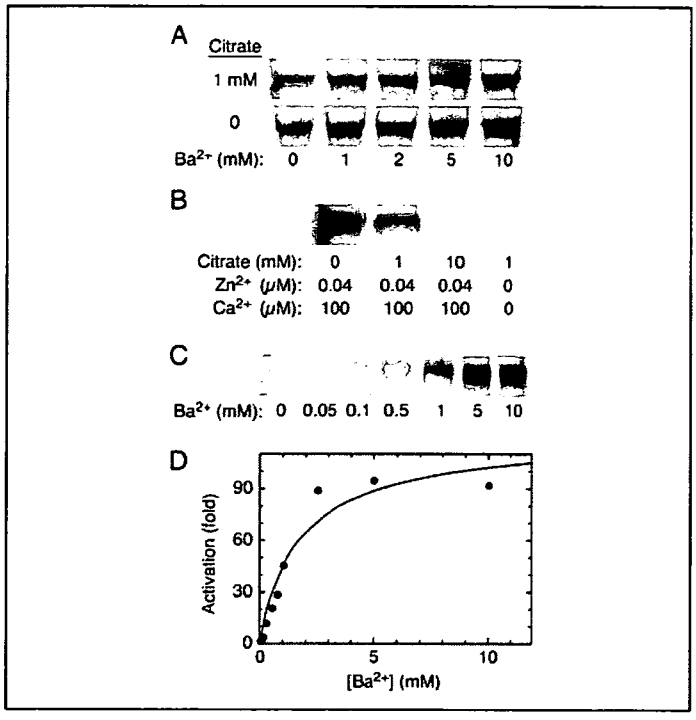

FIGURE 4. **Effects of citrate and barium ions on ADAMTS13 activity at low ionic strength.** A, plasma ADAMTS13 (0.6 nM) was assayed in 5 mM Hepes, pH 8.0, with VWF substrate (2 • g/ml) and increasing concentrations of barium ion with or without 1 mM sodium citrate. The 350 -kDa VWF cleavage product was detected by gel electrophoresis and Western blotting. B, effects of sodium citrate on recombinant ADAMTS13 (30 nM) in the presence and absence of zinc and calcium ions. C, recombinant ADAMTS13 (30 nM) was assayed as in A with increasing concentrations of barium ions and without sodium citrate. D, the activation (fold) of ADAMTS13 as a function of barium ion concentration was determined by chemifluorescence analysis of Western blots from several experiments including those in panel B. The maximum extent of VWF cleavage product formed was • 15% of total cleavable VWF all conditions. The line represents the least squares fit of the quadratic binding equation to the data using the parameters described in the text.

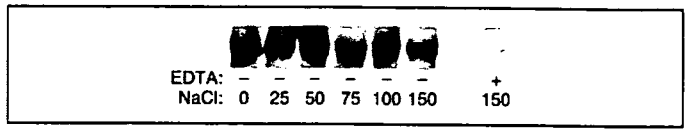

FIGURE 5. **Dependence of ADAMTS13 activity on ionic strength and sodium ion concentration.** Plasma ADAMTS13 was assayed in 50 mM Hepes, pH 7.4, 250 • M $ZnCl_2$, and 5 mM $CaCl_2$ with increasing concentrations of sodium chloride (mM) without (•) or with (•) 10 mM EDTA. The 350-kDa VWF cleavage product was detected by gel electrophoresis and Western blotting.

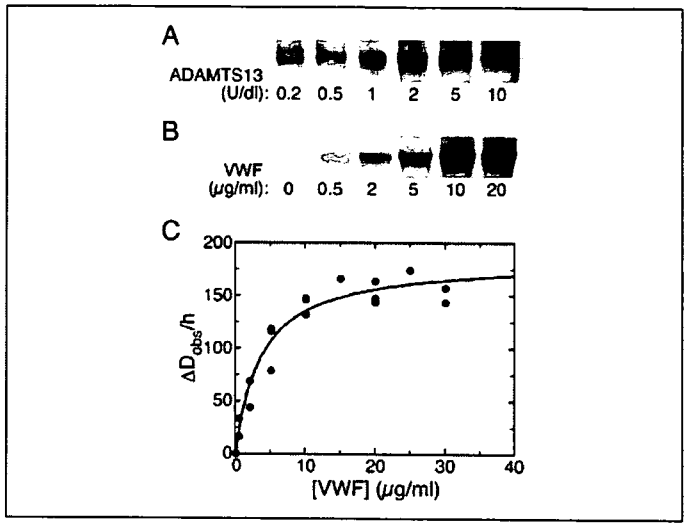

FIGURE 6. **Activity of ADAMTS13 at physiological pH and ionic strength.** A, the concentration of plasma ADAMTS13 was varied in reactions (1 h) containing 250 • M $ZnCl_2$, 5 mM $CaCl_2$, and a constant VWF concentration (20 • g/ml). B, the concentration of VWF was varied in reactions containing 250 • M $ZnCl_2$, 5 mM $CaCl_2$, and a constant ADAMTS13 concentration (0.6 nM). C, the densities of the 350-kDa product band as a function of VWF concentration were calculated from scanned films for the experiments performed as in B. The line represents the least squares fit of the Michaelis-Menten equation with the parameters described in the text. Under these conditions, VWF cleavage product generation was linear with time and • 15% of susceptible substrate was cleaved during the assay.

operate efficiently at physiological ionic strength. Therefore, the dependence of ADAMTS13 activity on ionic strength was investigated with optimal concentrations of zinc and calcium ions (Fig. 5). Under these conditions ADAMTS13 was fully active at ionic strengths up to I • 285 mM (including the contribution of ionized guanidine HCl). Several zinc metalloproteinases and serine proteinases have demonstrated a dependence on sodium ions for activity (33, 34). However, increasing concentrations of sodium chloride, maintaining constant ionic strength with choline chloride, did not alter ADAMTS13 activity (data not shown), indicating that sodium ions do not have a specific effect on ADAMTS13. The results indicate that high ionic strength does not necessarily inhibit ADAMTS13.

Kinetics of VWF Cleavage—The kinetic properties of ADAMTS13 were assessed under conditions approximating physiological pH, ionic strength, and concentrations of zinc and calcium ions. The purified VWF substrate was pretreated with 1.2 M guanidine HCl to induce a conformation susceptible to cleavage (5) and diluted 10-fold into the reaction. Proteolysis of VWF was dependent on both enzyme (Fig. 6A) and substrate concentrations (Fig. 6B). The rate of proteolysis displayed a hyperbolic dependence on VWF concentration with a $K_{m\ app}$ of 3.7 • 1.4 • g/ml, or 15 nM in VWF subunits (Fig. 6C). ADAMTS13 binds directly to surface-immobilized VWF with a $K_{D\ app}$ of • 4 • g/ml (35), and the concentration of VWF in plasma is • 5–10 • g/ml (36), suggesting that ADAMTS13 functions within a physiological substrate concentration range. The enzyme displayed exponential progress curves at a relatively low VWF concentration of 2 • g/ml (• 0.5 • $K_{m\ app}$), consistent with first order reaction kinetics and an apparent first order rate constant k_{obs} of 0.033 • 0.021 min^{-1} and $[VWF]_{max}$ of 0.34 • 0.07 • g/ml VWF cleaved (Fig. 7). These results indicate a value for k_{cat} of • 0.83 min^{-1}. This value must be considered a rough estimate because the generation of observed 350-kDa VWF cleavage product requires the cleavage of two adjacent subunits. Determining the true kinetic constants for VWF will require the use of an assay that measures the cleavage of single bonds. Control experiments showed that ADAMTS13 activity was stable for at least 3 h under reaction conditions. Thus, ADAMTS13 cleaves VWF efficiently under physiological conditions of pH, ionic strength, and metal ion concentration. However, a maximum of 14 • 5% of the total VWF substrate was susceptible to ADAMTS13.

The incomplete cleavage of VWF (Fig. 7) suggested that the substrate was heterogeneous in sensitivity to ADAMTS13 or became resistant during the course of the reaction. To distinguish these possibilities, VWF pretreated with guanidine HCl was diluted 10-fold into reaction buffer and incubated for 100 min prior to the addition of ADAMTS13. Similar reaction kinetics were observed, and a maximum of 6 • 2% of the substrate was cleaved (data not shown). Thus, the partial cleavage of VWF was reduced • 50% but not eliminated by preincubation without enzyme. The state of the uncleavable VWF is unclear. Denaturation with low concentrations of guanidine may never allow VWF to adopt a cleavable conformation, or upon dilution, some VWF may immediately refold and become resistant to ADAMTS13. These results are consistent with the effects of guanidine HCl on the cleavage of plasma VWF (5) and recombinant VWF (23) by highly purified plasma ADAMTS13.

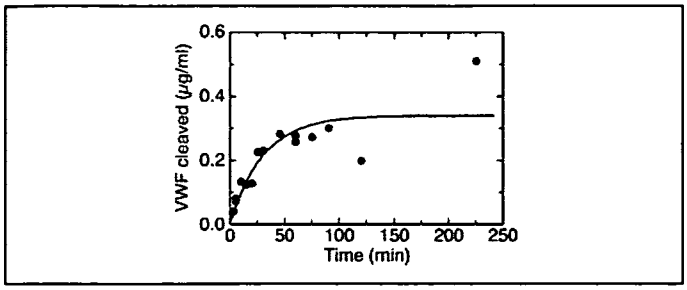

FIGURE 7. **Progress curve for ADAMTS13 cleavage of guanidine-treated VWF.** The concentration of VWF products as a function of time were calculated from the density of the 350-kDa product band by chemifluorescent detection. The reactions contained 2 • g/ml VWF and 0.6 nM plasma ADAMTS13 and were performed as described under "Experimental Procedures." The line represents the least squares fit of Equation 1 to the data with the parameters described in the text.

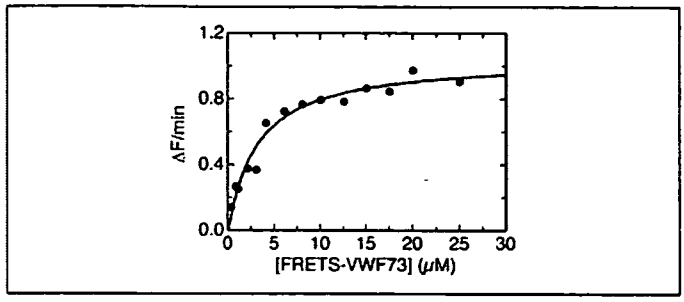

FIGURE 8. **ADAMTS13 cleavage of FRETS-VWF73.** The reactions were performed with 0.15 nM plasma ADAMTS13, and the observed rates of change in fluorescence intensity (• F/min) were analyzed as a function of FRETS-VWF73 concentration as described under "Experimental Procedures." Under these conditions, a product concentration of 2 • M corresponds to • 240 • F. The line represents the least squares fit of the Michaelis-Menten equation with the parameters described in the text.

FRETS-VWF73 Cleavage—The activity of ADAMTS13 toward a structurally homogeneous substrate was investigated using a fluorescent synthetic peptide, FRETS-VWF73, corresponding to residues Asp^{1596}–Arg^{1668} of VWF domain A2 and containing the Tyr^{1605}–Met^{1606} bond cleaved by ADAMTS13 (30). The reactions were performed at approximately physiological pH, ionic strength, and concentrations of zinc and calcium ions. Proteolysis of FRETS-VWF73 was linear with time up to 2 h (data not shown), confirming the stability of ADAMTS13 activity. The reaction demonstrated typical Michaelis-Menten kinetics, with a $K_{m\,app}$ of 3.2 • 1.1 • M and V_{max} of 1.04 • 0.10 • F/min, or a k_{cat} of • 58 min^{-1} (Fig. 8), which is • 70-fold greater than the k_{cat} for VWF cleavage of • 0.83 min^{-1}. The • 210-fold increase in $K_{m\,app}$ compared with multimeric VWF treated with guanidine HCl (Fig. 6) suggests that FRETS-VWF73 lacks tertiary structure or possibly exosites within full-length VWF that may be required for efficient substrate recognition.

The metal ion dependence of FRETS-VWF73 cleavage was qualitatively similar to that of VWF cleavage, although the $K_{D\,app}$ for calcium ion was higher. Activity was undetectable without added metal ions and was increased by calcium ions with a $K_{D\,app}$ of 60 • 25 • M. In the presence of 10 • M zinc ions, calcium supported a similar level of activity with a $K_{D\,app}$ of 74 • 35 • M (Fig. 9A). Zinc ions alone stimulated ADAMTS13 activity at concentrations • 20 • M, but higher concentrations were markedly inhibitory. In the presence of optimal calcium ions, concentrations of zinc ion • 10 • M supported full activity, and higher concentrations were inhibitory (Fig. 9B).

Barium ions also stimulated the cleavage of FRETS-VWF73 (2 • M). Normalized to the maximal activity with 10 • M zinc and 1.5 mM calcium ions (100%), the activity observed with 10 mM barium ions was 66%, and that with 10 mM barium plus 10 • M zinc ions was 89%.

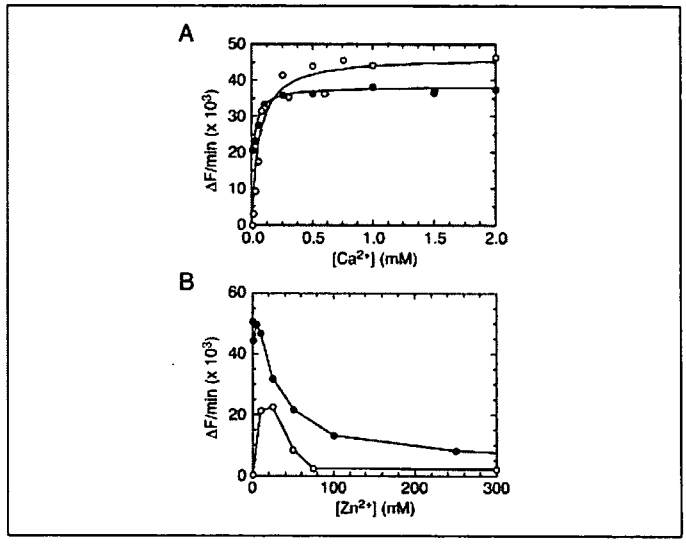

FIGURE 9. **FRETS-VWF73 cleavage by recombinant ADAMTS13 and metal ions.** The assays contained 0.3 nM recombinant ADAMTS13, 2 • M FRETS-VWF73, and various metal ion concentrations. The observed rates of change in fluorescence intensity (• F/min) were analyzed as a function of FRETS-VWF73 concentration as described under "Experimental Procedures." The values for • F/min were measured on a different fluorometer and cannot be compared with those in Fig. 8. A, reactions were performed with the indicated concentration of calcium ions in the absence (open circles) or presence (filled circles) of 10 • M zinc ions. The lines represent the least squares fit of the quadratic binding equation with the parameters described in the text. B, reactions were performed with the indicated concentration of calcium ions in the absence (open circles) or presence (filled circles) of 5 mM calcium ions.

DISCUSSION

ADAMTS13 shares several metal ion binding properties with other metalloproteinases. The active site zinc ion of ADAMTS13 binds to the sequence ^{224}HEXXHXXGXXHD^{235} (1), which is common among other metalloproteinases including members of the matrix metalloproteinases and the ADAM families (18, 19, 37). For some metalloproteinases, divalent cations other than zinc can support catalytic activity. For example, reconstitution of apo-stromelysin (MMP-3) with cobalt ions restored the activity by 80% (38), and reconstitution of apo-matrilysin (MMP-7) with manganese, nickel, or cobalt ions also restored activity (39, 40). In addition, calcium, magnesium, and manganese ions have been demonstrated to support procollagen N-proteinase (ADAMTS2) activity, whereas copper and high concentrations of zinc ions inhibit the enzyme (41, 42). Cobalt or copper ions supported the catalytic activity of astacin, and the crystal structure showed that these ions had pentagonal bipyriamidal coordination states similar to that of the catalytic zinc ion in native astacin. In contrast, mercury or nickel ions displayed different coordination geometries and inhibited the enzyme (43). In the present study, copper ions slightly enhanced the activity of ADAMTS13, whereas nickel ions inhibited the enzyme and cobalt ions had no effect (Fig. 1). These results are broadly similar to the divalent metal ion effects reported previously for plasma ADAMTS13 under somewhat different assay conditions including pH 8.0, 1 M urea and low ionic strength (4). Additional experiments will be necessary to determine whether divalent metal ions other than zinc can support ADAMTS13 enzyme activity.

Like several other metalloproteinases, ADAMTS13 is inhibited by excessively high concentrations of zinc ions, perhaps because of the formation of $Zn(OH)^+$ that binds to the catalytic Glu or Asp residue within the active site. For example, carboxypeptidase A is inhibited by zinc ions with a K_i of 24 • M (31). The amount of added zinc ions required to activate or inactivate ADAMTS13 depends on the concentration of metal ion chelators. In reactions containing 1 mM EDTA,

plasma ADAMTS13 was reported to be fully active with 2 mM total zinc ions but inactive with 3 mM zinc ions (23). In the present study, ADAMTS13 in citrated plasma was activated at least • 2-fold by 1 mM zinc ions but was inactive at concentrations • 3 mM (Fig. 1), whereas recombinant ADAMTS13 with no added chelators was activated • 200-fold by 5 • M zinc ions (Figs. 3 and 9) and inactivated by • 50 • M zinc ions (Fig. 9). This exquisite sensitivity to inhibition by excess zinc ions suggests that ADAMTS13 assays should precisely control the free concentrations of divalent metal ions, particularly in assays developed for clinical use.

Calcium ions play a structural role in many metalloproteinases and stimulate ADAMTS13 activity (4, 5, 23), suggesting a functional interaction between zinc and calcium ion binding. Calcium ions dramatically activate recombinant ADAMTS13 cleavage of VWF and bind with a $K_{D\,app}$ of • 4.8 • M (Fig. 3), well below the plasma free calcium ion concentration of • 1.2 mM. The $K_{D\,app}$ was significantly higher, • 60 • M, when assayed with the FRETS-VWF73 peptide substrate (Fig. 9A). The cause of this difference is not known. Although not studied in detail, the ability of calcium ions alone to stimulate ADAMTS13, a putative zinc-dependent metalloprotease, implies that a very low concentration of zinc ions is present in the dialyzed recombinant enzyme preparations used in these studies (Figs. 3D and 9A) and suggests that zinc and calcium ions bind cooperatively to ADAMTS13. Molecular modeling based on the crystal structures of adamalysin II (44) and ADAM33 (45), which are homologous to ADAMTS13, indicates that calcium ion- and zinc ion-binding sites are located on opposites sides of the ADAMTS13 metalloprotease domain, separated by • 24 Å (1) (data not shown). Therefore, cooperative interactions between the zinc and calcium ions must be mediated indirectly through changes in protein structure. Studies using apo-ADAMTS13 will need to be performed to further establish the role of zinc and calcium ions in the activity of ADAMTS13.

Barium and strontium ions reportedly are more potent than calcium ions for activating ADAMTS13, and clinical ADAMTS13 assays frequently employ supplementation with barium ions (4, 5). The stimulation of ADAMTS13 activity might be due to the occupancy of calcium-binding sites by barium ions, but this explanation probably is incomplete. At low ionic strength (I • 2.5 to 22.5 mM), ADAMTS13 activity in citrated plasma was enhanced • 2-fold by 5–10 mM barium ions (Fig. 4). In contrast, under conditions of physiological ionic strength and pH, the addition of increasing concentrations of barium ions had little or no effect on the activity of ADAMTS13 in citrated plasma (Fig. 1). Barium ions did not enhance ADAMTS13 activity in plasma that was free of citrate (Fig. 4A) and did not stimulate recombinant ADAMTS13 when present at concentrations comparable with the maximally effective concentrations of calcium ions (Fig. 4C). However, much higher levels of barium ions (• 5 mM) did stimulate recombinant ADAMTS13 activity (Fig. 4D), suggesting that barium ions can occupy the calcium ion site on ADAMTS13 but with substantially lower affinity. Citrate also inhibits the calcium- and zinc-dependent activity of ADAMTS13 (Fig. 4B). Consequently, the ability of barium ions to activate ADAMTS13 in citrated plasma samples probably is due to the displacement of more potent calcium or zinc ions from complexes with citrate.

These results suggest that sodium citrate is not the optimal anticoagulant for assays of ADAMTS13 activity in blood samples. ADAMTS13 activity is normal in heparinized plasma (5),[4] suggesting that heparin might be an acceptable nonchelating substitute for citrate. Alternatively, anticoagulation may be dispensable because ADAMTS13 appears to be recovered quantitatively in serum (4).

ADAMTS13 is inhibited markedly by increasing ionic strength when assayed in the presence of 1–1.5 M urea (4, 46). However, little or no effect of ionic strength is observed in the absence of urea. Guanidine HCl induces a VWF conformation that is susceptible to ADAMTS13 but also relatively stable after the guanidine HCl concentration is reduced by dilution. The cleavage of guanidine-treated VWF is insensitive to sodium chloride (Fig. 5) or choline chloride (data not shown), indicating that the binding of ADAMTS13 to this form of the substrate does not depend strongly on ionic strength. Although the reaction conditions in these studies vary in other ways that could be significant, a primary role for urea in causing the differences is consistent with the well characterized ability of ionic strength to stabilize proteins against denaturation by urea (47, 48). Consequently, neutral salts like sodium chloride may simply prevent urea-induced changes in the conformation of the VWF substrate that would make it susceptible to ADAMTS13. This conclusion is supported by changes in VWF conformation induced by physiological concentrations of sodium chloride and by other sodium salts, as monitored by intrinsic protein fluorescence (46).

The cleavage of the small fragment of VWF contained in FRETS-VWF73 is relatively insensitive to ionic strength (49) and does not require denaturants (30, 49). This isolated fragment also lacks significant secondary structure by NMR spectroscopy (50). These findings are consistent with the following model in which urea and ionic strength interact and modulate the cleavage of native VWF by ADAMTS13; the transition from a resistant to a susceptible conformation of VWF is facilitated by urea and inhibited by neutral salts, but the recognition and cleavage of the susceptible VWF conformation is largely independent of ionic strength.

Although FRETS-VWF73 does not require denaturation to be cleaved by ADAMTS13, guanidine-treated VWF has a • 210-fold lower $K_{m\,app}$ (Fig. 8). This discrepancy implies that ADAMTS13 interacts with specific, extended structural features of multimeric VWF. Molecular modeling of the A2 domain suggests that it has a characteristic • /• -fold with a six-stranded • -sheet surrounded by three • -helices on each side. The Tyr^{1605}–Met^{1606} peptide bond is predicted to be buried within the • -sheet, supporting the need for large conformational changes of the A2 domain prior to proteolysis (51, 52). Efficient cleavage also requires the segment Glu^{1660}–Arg^{1668} in the C-terminal • -helix of the A2 domain (49). The fragment of VWF represented in FRETS-VWF73 corresponds to approximately three • -strands and three • -helices of the A2 domain, but when removed from the context of the complete domain this isolated peptide has no distinct secondary structure (50). Therefore, the relatively poor $K_{m\,app}$ value for FRETS-VWF73 may reflect the large entropic cost of adopting a conformation that can bind ADAMTS13. In addition, such a small fragment of the A2 domain may lack additional sites on VWF that interact with ADAMTS13. For example, the adjacent A1 domain may bind cofactors that affect cleavage (53), and the A3 domain may provide a docking site for ADAMTS13 (54). Such interactions may explain why VWF has both a • 210-fold lower $K_{m\,app}$ and a • 70-fold lower k_{cat} than FRETS-VWF73. These changes have the effect of minimizing the difference in catalytic efficiency ($k_{cat}/K_{m\,app}$) between VWF (55 • M^{-1} min^{-1}) and FRETS-VWF73 (18 • M^{-1} min^{-1}). These kinetic constants must be compared cautiously because the values for VWF are distorted by heterogeneity of the substrate and the complexity of the assay. Nevertheless, independent measurements of ADAMTS13 binding to immobilized VWF (35) yielded an equilibrium constant (K_D • 14 nM, per subunit of VWF) similar to the $K_{m\,app}$ for VWF cleavage of 15 nM.

[4] E. A. Tuley and P. J. Anderson, unpublished results.

These studies demonstrate that both plasma and recombinant ADAMTS13 function efficiently under physiological conditions. Once VWF adopts a suitable conformation, perhaps under the influence of fluid shear stress, ADAMTS13 can cleave it rapidly at the pH levels, ionic strengths, and divalent metal ion concentrations that prevail in vivo. The ionic strength and denaturant concentrations that are optimal for ADAMTS13 assays in vitro, in the absence of fluid shear stress, promote conformational changes in VWF necessary to make it susceptible to cleavage. However, these nonphysiological conditions may impair the recognition of susceptible VWF by ADAMTS13.

The effect of calcium or barium ions on ADAMTS13 activity probably reflects binding to a structural metal ion site in the metalloprotease domain, as predicted by molecular modeling (1) The VWF substrate also might bind calcium ions, but this has not been reported. The VWF A1, A2, and A3 domains do not have MIDAS metal ion sites found in the homologous A domains of certain integrin subunits, and the crystal structures of the VWF A1 and A3 domains do not show metal ions (55, 56). Whether other VWF domains bind metal ions is unknown. Calcium ions are required for optimal cleavage of the FRETS-VWF73 peptide substrate (Fig. 9), which is disordered in solution (50) and presumably unable to bind calcium ions with high affinity. Therefore, calcium ions probably bind directly to ADAMTS13 to stimulate substrate cleavage. Although one calcium site is likely to be in the metalloprotease domain, additional sites in other domains cannot be excluded. For example, the CUB domains in complement component C1s have well defined calcium binding sites (57), suggesting that the two C-terminal CUB domains of ADAMTS13 might have similar sites. Detailed understanding of how ADAMTS13 regulates platelet adhesion should be facilitated by further characterization of the requirements for substrate exposure and recognition by ADAMTS13.

Acknowledgments—We thank Claudine Mazurier (Laboratoire Français du Fractionnement et des Biotechnologies, Lille, France) for the generous gift of purified VWF, Mary Burritt and John Butz (Mayo Clinic, Rochester, MN) for performing inductively coupled plasma spectroscopy analyses, and Paul E. Bock (Vanderbilt University School of Medicine) for helpful discussions of data analysis.

REFERENCES

1. Zheng, X., Chung, D., Takayama, T. K., Majerus, E. M., Sadler, J. E., and Fujikawa, K. (2001) J. Biol. Chem. **276,** 41059–41063
2. Levy, G. G., Nichols, W. C., Lian, E. C., Foroud, T., McClintick, J. N., McGee, B. M., Yang, A. Y., Siemieniak, D. R., Stark, K. R., Gruppo, R., Sarode, R., Shurin, S. B., Chandrasekaran, V., Stabler, S. P., Sabio, H., Bouhassira, E. E., Upshaw, J. D., Jr., Ginsburg, D., and Tsai, H. M. (2001) Nature **413,** 488–494
3. Soejima, K., Mimura, N., Hirashima, M., Maeda, H., Hamamoto, T., Nakagaki, T., and Nozaki, C. (2001) J. Biochem. (Tokyo) **130,** 475–480
4. Furlan, M., Robles, R., and Lammle, B. (1996) Blood **87,** 4223–4234
5. Tsai, H. M. (1996) Blood **87,** 4235–4244
6. Tsai, H. M., and Lian, E. C. (1998) N. Engl. J. Med. **339,** 1585–1594
7. Ruggeri, Z. M. (2003) J. Thromb. Haemostasis **1,** 1335–1342
8. Sadler, J. E. (1998) Annu. Rev. Biochem. **67,** 395–424
9. Kokame, K., Matsumoto, M., Soejima, K., Yagi, H., Ishizashi, H., Funato, M., Tamai, H., Konno, M., Kamide, K., Kawano, Y., Miyata, T., and Fujimura, Y. (2002) Proc. Natl. Acad. Sci. U. S. A. **99,** 11902–11907
10. Moake, J. L. (2004) Semin. Hematol. **41,** 4–14
11. Rock, G. A., Shumak, K. H., Buskard, N. A., Blanchette, V. S., Kelton, J. G., Nair, R. C., and Spasoff, R. A. (1991) N. Engl. J. Med. **325,** 393–397
12. Rock, G., Porta, C., and Bobbio-Pallavicini, E. (2000) Haematologica **85,** 410–419
13. Zheng, X. L., Kaufman, R. M., Goodnough, L. T., and Sadler, J. E. (2004) Blood **103,** 4043–4049
14. Tang, B. L. (2001) Int. J. Biochem. Cell Biol. **33,** 33–44
15. Nagase, H., and Kashiwagi, M. (2003) Arthritis Res. Ther. **5,** 94–103
16. Moake, J. L., Turner, N. A., Stathopoulos, N. A., Nolasco, L. H., and Hellums, J. D. (1986) J. Clin. Invest. **78,** 1456–1461
17. Bork, P., and Beckmann, G. (1993) J. Mol. Biol. **231,** 539–545
18. Bode, W., Gomis-Ruth, F. X., and Stockler, W. (1993) FEBS Lett. **331,** 134–140
19. Stocker, W., Grams, F., Baumann, U., Reinemer, P., Gomis-Ruth, F. X., McKay, D. B., and Bode, W. (1995) Protein Sci. **4,** 823–840
20. Vallee, B. L., and Auld, D. S. (1990) Biochemistry **29,** 5647–5659
21. Auld, D. S. (2001) Biometals **14,** 271–313
22. Chung, D. W., and Fujikawa, K. (2002) Biochemistry **41,** 11065–11070
23. Tsai, H.-M., Sussman, I. I., Ginsburg, D., Lankhof, H., Sixma, J. J., and Nagel, R. L. (1997) Blood **89,** 1954–1962
24. Girma, J. P., Chopek, M. W., Titani, K., and Davie, E. W. (1986) Biochemistry **25,** 3156–3163
25. Zheng, X., Nishio, K., Majerus, E. M., and Sadler, J. E. (2003) J. Biol. Chem. **278,** 30136–30141
26. Majerus, E. M., Zheng, X., Tuley, E. A., and Sadler, J. E. (2003) J. Biol. Chem. **278,** 46643–46648
27. Bock, P. E., Olson, S. T., and Bjork, I. (1997) J. Biol. Chem. **272,** 19837–19845
28. Rand, M., Lock, J., van't Veer, C., Gaffney, D., and Mann, K. (1996) Blood **88,** 3432–3445
29. Segel, I. H. (1975) Enzyme Kinetics: Behavior and Analysis of Rapid Equilibrium and Steady State Enzyme Systems, Wiley, pp. 39–44, New York
30. Kokame, K., Nobe, Y., Kokubo, Y., Okayama, A., and Miyata, T. (2005) Br. J. Haematol. **129,** 93–100
31. Auld, D. S. (1995) Methods Enzymol. **248,** 228–242
32. Gerritsen, H. E., Turecek, P. L., Schwarz, H. P., Lammle, B., and Furlan, M. (1999) Thromb. Haemostasis **82,** 1386–1389
33. Inouye, K., Lee, S. B., and Tonomura, B. (1996) Biochem. J. **315,** 133–138
34. Rose, T., and Di Cera, E. (2002) J. Biol. Chem. **277,** 19243–19246
35. Majerus, E. M., Anderson, P. J., and Sadler, J. E. (2005) J. Biol. Chem. **280,** 21773–21778
36. Chopek, M. W., Girma, J. P., Fujikawa, K., Davie, E. W., and Titani, K. (1986) Biochemistry **25,** 3146–3155
37. Bode, W., and Maskos, K. (2003) Biol. Chem. **384,** 863–872
38. Salowe, S. P., Marcy, A. I., Cuca, G. C., Smith, C. K., Kopka, I. E., Hagmann, W. K., and Hermes, J. D. (1992) Biochemistry **31,** 4535–4540
39. Cha, J., Pedersen, M. V., and Auld, D. S. (1996) Biochemistry **35,** 15831–15838
40. Cha, J., Sorensen, M. V., Ye, Q.-Z., and Auld, D. S. (1998) J. Biol. Inorg. Chem. **3,** 353–359
41. Tuderman, L., Kivirikko, K. I., and Prockop, D. J. (1978) Biochemistry **17,** 2948–2954
42. Hojima, Y., Behta, B., Romanic, A. M., and Prockop, D. J. (1994) Matrix Biol **14,** 113–120
43. Gomis-Ruth, F. X., Grams, F., Yiallouros, I., Nar, H., Kusthardt, U., Zwilling, R., Bode, W., and Stocker, W. (1994) J. Biol. Chem. **269,** 17111–17117
44. Gomis-Ruth, F. X., Kress, L. F., Kellermann, J., Mayr, I., Lee, X., Huber, R., and Bode, W. (1994) J. Mol. Biol. **239,** 513–544
45. Orth, P., Reichert, P., Wang, W., Prosise, W. W., Yarosh-Tomaine, T., Hammond, G., Ingram, R. N., Xiao, L., Mirza, U. A., Zou, J., Strickland, C., Taremi, S. S., Le, H. V., and Madison, V. (2004) J. Mol. Biol. **335,** 129–137
46. De Cristofaro, R., Peyvandi, F., Palla, R., Lavoretano, S., Lombardi, R., Merati, G., Romitelli, F., Di Stasio, E., and Mannucci, P. M. (2005) J. Biol. Chem. **280,** 23295–23302
47. Yao, M., and Bolen, D. W. (1995) Biochemistry **34,** 3771–3781
48. Maldonado, S., Irun, M. P., Campos, L. A., Rubio, J. A., Luquita, A., Lostao, A., Wang, R., Garcia-Moreno, E. B., and Sancho, J. (2002) Protein Sci. **11,** 1260–1273
49. Kokame, K., Matsumoto, M., Fujimura, Y., and Miyata, T. (2004) Blood **103,** 607–612
50. Sadler, J. E., Moake, J. L., Miyata, T., and George, J. N. (2004) Hematology (Am. Soc. Hematol. Educ. Program), 407–423
51. Jenkins, P. V., Pasi, K. J., and Perkins, S. J. (1998) Blood **91,** 2032–2044
52. Sutherland, J. J., O'Brien, L. A., Lillicrap, D., and Weaver, D. F. (2004) J. Mol. Model. **10,** 259–270
53. Nishio, K., Anderson, P. J., Zheng, X. L., and Sadler, J. E. (2004) Proc. Natl. Acad. Sci. U. S. A. **101,** 10578–10583
54. Dong, J.-F., Moake, J. L., Bernardo, A., Fujikawa, K., Ball, C., Nolasco, L., Lopez, J. A., and Cruz, M. A. (2003) J. Biol. Chem. **278,** 29633–29639
55. Emsley, J., Cruz, M., Handin, R., and Liddington, R. (1998) J. Biol. Chem. **273,** 10396–10401
56. Bienkowska, J., Cruz, M., Atiemo, A., Handin, R., and Liddington, R. (1997) J. Biol. Chem. **272,** 25162–25167
57. Gregory, L. A., Thielens, N. M., Arlaud, G. J., Fontecilla-Camps, J. C., and Gaboriaud, C. (2003) J. Biol. Chem. **278,** 32157–32164